NAVAL POSTGRADUATE SCHOOL

MONTEREY, CALIFORNIA

THESIS

SIMULATION PERFORMANCE OF MULTIPLE-INPUT MULTIPLE-OUTPUT SYSTEMS EMPLOYING SINGLE-CARRIER MODULATION AND ORTHOGONAL FREQUENCY DIVISION MULTIPLEXING

by

Halil Derya Saglam

December 2004

Thesis Advisor:	Murali Tummala
Co-Advisor:	Roberto Cristi

Approved for public release; distribution is unlimited

THIS PAGE INTENTIONALLY LEFT BLANK

REPORT DOCUMENTATION PAGE		Form Approved OMB No. 0704-0188
Public reporting burden for this collection of information is estimated to average 1 hour per response, including the time for reviewing instruction, searching existing data sources, gathering and maintaining the data needed, and completing and reviewing the collection of information. Send comments regarding this burden estimate or any other aspect of this collection of information, including suggestions for reducing this burden, to Washington headquarters Services, Directorate for Information Operations and Reports, 1215 Jefferson Davis Highway, Suite 1204, Arlington, VA 22202-4302, and to the Office of Management and Budget, Paperwork Reduction Project (0704-0188) Washington DC 20503.		
1. AGENCY USE ONLY ***(Leave blank)***	**2. REPORT DATE** December 2004	**3. REPORT TYPE AND DATES COVERED** Master's Thesis
4. TITLE AND SUBTITLE: Simulation Performance of Multiple-Input Multiple-Output Systems Employing Single-Carrier Modulation And Orthogonal Frequency Division Multiplexing		**5. FUNDING NUMBERS**
6. AUTHOR(S) Halil Derya Saglam		
7. PERFORMING ORGANIZATION NAME(S) AND ADDRESS(ES) Naval Postgraduate School Monterey, CA 93943-5000		**8. PERFORMING ORGANIZATION REPORT NUMBER**
9. SPONSORING /MONITORING AGENCY NAME(S) AND ADDRESS(ES) N/A		**10. SPONSORING/MONITORING AGENCY REPORT NUMBER**
11. SUPPLEMENTARY NOTES The views expressed in this thesis are those of the author and do not reflect the official policy or position of the Department of Defense or the U.S. Government.		
12a. DISTRIBUTION / AVAILABILITY STATEMENT Approved for public release; distribution is unlimited		**12b. DISTRIBUTION CODE**

13. ABSTRACT (maximum 200 words)

This thesis investigates the simulation performance of multiple-input multiple-output (MIMO) systems utilizing Alamouti-based space-time block coding (STBC) technique. The MIMO communication systems using STBC technique employing both single-carrier modulation and orthogonal frequency division multiplexing (OFDM) are simulated in Matlab. The physical layer part of the IEEE 802.16a standard is used in constructing the simulated OFDM schemes. Stanford University Interim (SUI) channel models are selected for the wireless channel in the simulation process. The performance results of the simulated MIMO systems are compared to those of conventional single antenna systems.

14. SUBJECT TERMS. Multiple-Input Multiple-Output (MIMO), Orthogonal Frequency Division Multiplexing (OFDM), Space-Time Block Coding (STBC), Stanford University Interim (SUI) Models, Spatially Correlated MIMO Channels, Spatial Diversity, Alamouti Scheme, Maximal Ratio Combining	**15. NUMBER OF PAGES** 93
	16. PRICE CODE

17. SECURITY CLASSIFICATION OF REPORT	**18. SECURITY CLASSIFICATION OF THIS PAGE**	**19. SECURITY CLASSIFICATION OF ABSTRACT**	**20. LIMITATION OF ABSTRACT**
Unclassified	Unclassified	Unclassified	UL

NSN 7540-01-280-5500

Standard Form 298 (Rev. 2-89)
Prescribed by ANSI Std. 239-18

THIS PAGE INTENTIONALLY LEFT BLANK

Approved for public release; distribution is unlimited

SIMULATION PERFORMANCE OF MULTIPLE-INPUT MULTIPLE-OUTPUT SYSTEMS EMPLOYING SINGLE-CARRIER MODULATION AND ORTHOGONAL FREQUENCY DIVISION MULTIPLEXING

Halil Derya Saglam
Lieutenant Junior Grade, Turkish Navy
B.S., Turkish Naval Academy, 1999

Submitted in partial fulfillment of the
requirements for the degree of

MASTER OF SCIENCE IN ELECTRICAL ENGINEERING

from the

NAVAL POSTGRADUATE SCHOOL
December 2004

Author: Halil Derya Saglam

Approved by: Murali Tummala
Thesis Advisor

Roberto Cristi
Co-Advisor

John Powers
Chairman, Department of Electrical and Computer Engineering

THIS PAGE INTENTIONALLY LEFT BLANK

ABSTRACT

This thesis investigates the simulation performance of multiple-input multiple-output (MIMO) systems utilizing Alamouti-based space-time block coding (STBC) technique. The MIMO communication systems using STBC technique employing both single-carrier modulation and orthogonal frequency division multiplexing (OFDM) are simulated in Matlab. The physical layer part of the IEEE 802.16a standard is used in constructing the simulated OFDM schemes. Stanford University Interim (SUI) channel models are selected for the wireless channel in the simulation process. The performance results of the simulated MIMO systems are compared to those of conventional single antenna systems.

THIS PAGE INTENTIONALLY LEFT BLANK

TABLE OF CONTENTS

LIST OF FIGURES

THIS PAGE INTENTIONALLY LEFT BLANK

LIST OF TABLES

THIS PAGE INTENTIONALLY LEFT BLANK

LIST OF ACRONYMS AND ABBREVIATIONS

AWGN	Additive White Gaussian Noise
BER	Bit Error Rate
CSI	Channel State Information
dB	decibel
FFT	Fast Fourier Transform
IFFT	Inverse Fast Fourier Transform
ISI	Inter Symbol Interference
MIMO	Multiple Input Multiple Output
MISO	Multiple Input Single Output
MRC	Maximal Ratio Combining
OFDM	Orthogonal Frequency Division Multiplexing
PSK	Phase Shift Keying
QAM	Quadrature Amplitude Modulation
RF	Radio Frequency
SC	Single Carrier
SIMO	Single Input Multiple Output
SISO	Single Input Single Output
STBC	Space Time Block Coding
SUI	Stanford University Interim

THIS PAGE INTENTIONALLY LEFT BLANK

ACKNOWLEDGEMENTS

I thank my wife Cigdem for being in my life and for the support and love she has given during my studies at NPS.

Thanks go out as well to Ruth and Bobby Moorhatch. The support and love you gave us will never be forgotten.

Finally, I want to thank my advisor Prof. Murali Tummala for his guidance and patience during the development of this thesis.

THIS PAGE INTENTIONALLY LEFT BLANK

EXECUTIVE SUMMARY

Future military and commercial wireless communication systems are required to provide higher data rates and reliable communication. Two major challenges in system design are the limited spectrum and the fading caused by multipath components in the wireless channel. To obtain higher data rates, larger bandwidths are required. To keep the same reliability under severe channel conditions, a higher transmitted power level is necessary. The emerging multiple-input multiple-output (MIMO) communication technologies have the potential to improve the performance without increasing the bandwidth or the transmitted power. MIMO systems exploit spatial diversity by employing multiple antennas at either side of the communication link. MIMO systems may add robustness to future military communication systems under battlefield conditions.

Due to its robustness under frequency selective channels, orthogonal frequency division multiplexing (OFDM) has been adopted in several wireless communication standards, such as the IEEE 802.11a local area network (LAN) standard and the IEEE 802.16a metropolitan area network (MAN) standard.

The combination of OFDM and MIMO technologies is a potential candidate for future wireless systems. When the spatial diversity gain provided by a MIMO system is added to robustness to fading provided by the OFDM systems, the performance of the resulting system is significantly enhanced compared to the conventional single antenna and single-carrier systems.

The main objective of this thesis was to investigate MIMO and MIMO-OFDM systems. The space coding techniques and the decoding algorithms studied in this thesis are based on the widely accepted Alamouti scheme. The Alamouti scheme was originally proposed for flat fading channels. The extended scheme, space-time block coding (STBC), has been developed for frequency-selective, multipath channels. The STBC technique is investigated for systems employing both single-carrier and OFDM modulation. Systems with two transmit antennas and a single receive antenna are the most investigated schemes utilizing the Alamouti and the STBC MIMO technique. By extending the

existing results for this case, in this thesis, we developed the input-output relations and decoding equations for the other possible antenna combinations, such as one transmitting and two receiving antennas, and two transmitting and two receiving antennas.

The widely used Stanford University Interim (SUI) channel models were selected to represent the wireless channel. The use of multiple antennas at both ends of a communication system results in multiple channels between the transmitter and the receiver. The multiple channels of MIMO systems are constructed using the SUI channel models. In practice, the spacing between antennas and the environment effects (angle of arrival and angle of departure of the electromagnetic waves) may cause correlation between these multiple channels. We investigated the spatial correlation effects on both frequency-flat and frequency-selective MIMO channels.

The MIMO systems with single-carrier and OFDM modulation were simulated in Matlab. Simulation results are presented in the form of the bit error rate (BER) curves. A performance comparison among the various MIMO systems is reported.

The most significant result of the simulations was that the systems employing higher number of antennas at either side of the communication link performed better than the ones with fewer antennas. In the work reported here, the best performing system was the MIMO-OFDM system with two transmitting and two receiving antennas. In a simulation using the SUI-2 channel model, at a BER of 10^{-4}, MIMO-OFDM performed 12 dB better than the conventional single antenna system employing single-carrier modulation; the total transmitted power was kept at the same level in each scheme.

I. INTRODUCTION

One of the biggest challenges in wireless communication is to operate in a time-varying multipath fading environment under limited power constraints. The other challenge is the limited availability of the frequency spectrum. Future commercial and military wireless systems will be required to support higher data rates with reliable communication under spectrum limitations and multipath fading environments. Military communication systems must maintain reliable communication under the conditions of hostile jamming and other interference without increasing emitted power or requiring larger bandwidth.

In order to improve the reliability without increasing the emitted power, time, frequency or space diversity could be exploited. In time diversity, the received signal is sampled at a higher rate, thus providing more than one sample per transmitted symbol. In frequency diversity, the same information is sent over a number of carriers [1]. Both diversity techniques require larger bandwidth. To exploit space diversity, the same information is transmitted or received through multiple antennas. Employing multiple antennas at the receiver and/or the transmitter improves the quality of a wireless communication link without increasing the transmitted power or bandwidth [2]. Therefore, the design and implementation of multiple-input multiple-output (MIMO) communication systems is an attractive research area.

Orthogonal frequency division multiplexing (OFDM) is a widely used method in wireless communication systems. Due to its effectiveness in multipath channel conditions, OFDM has been adopted by several wireless communication standards, such as the IEEE 802.11a local area network (LAN) standard and the IEEE 802.16a metropolitan area network (MAN) standard. The combination of OFDM and MIMO systems presents better solutions by adding more diversity gain to the conventional OFDM systems employing a single antenna at both the receiver and the transmitter [3]. The robustness to fading provided by OFDM is enhanced by the spatial diversity of MIMO systems, and the resulting performance of MIMO-OFDM systems is significantly improved.

A. OBJECTIVE AND METHODOLOGY

The main objective of this thesis was to investigate MIMO and MIMO-OFDM systems and compare their performance to the conventional single antenna systems. The first step to achieve this goal was to study the fundamentals of MIMO systems by investigating their performance in a communication system. In this thesis, the published techniques for the systems with single-carrier modulation and with OFDM were investigated. Several communication systems with various numbers of antennas utilizing both single-carrier modulation and OFDM were developed in Matlab. The developed systems were simulated using the widely used Stanford University Interim (SUI) channel models.

B. RELATED RESEARCH

Due to their efficiency in providing an improved performance without increasing the bandwidth or the emitted power, MIMO systems are the subject of considerable research effort. Probably the most attractive scheme from the stand point of implementation and performance is the Alamouti's transmit diversity scheme [4] based on maximal ratio combining (MRC) [5]. Numerous studies have been performed to investigate its performance and led to the development of several variations [6, 7]. The scheme was originally developed for flat fading channels. Subsequently, it has been extended to frequency selective channel cases [8, 9] and renamed as "the space-time block coding (STBC) technique". Later, the extended scheme has been selected to be a part of the IEEE 802.16a standard [10].

Channel modeling is another research area in MIMO systems. The IEEE 802.16 Broadband Wireless Access Working Group proposed SUI channel models for system simulation [11]. The presented channel models have been widely used by many research studies.

C. ORGANIZATION OF THE THESIS

This thesis is organized into six chapters. Chapter II introduces the input-output relations in MIMO systems and Alamouti's transmit diversity scheme designed for flat fading channels. Chapter III introduces the SUI channel models. The uncorrelated MIMO channels based on SUI modeling and their extension to correlated MIMO channels are

also discussed. Chapter IV introduces the STBC scheme that uses both single-carrier modulation and OFDM. Chapter V presents the simulation results of the communication systems developed in Matlab. Chapter VI provides a summary of the work, the conclusions and suggestions for future studies.

Appendix A lists the SUI channel parameters. Appendix B provides an explanation of the Matlab simulation.

THIS PAGE INTENTIONALLY LEFT BLANK

II. MIMO SYSTEMS AND ALAMOUTI SCHEME

The goal of this chapter is to introduce a widely used space coding technique called the Alamouti scheme. An overview of the input-output relations of MIMO systems is presented to describe the space coding algorithm at the transmitter and the decoding process at the receiver in the Alamouti scheme.

A. MULTIPLE-INPUT MULTIPLE-OUTPUT (MIMO) SYSTEMS

In order to develop the input-output relations of single-input multiple-output (SIMO), multiple-input single-output (MISO) and MIMO systems, the single-input single-output (SISO) system is described first.

1. Single-Input Single-Output (SISO) Systems

The schematic diagram of a SISO system is shown in Figure 1. The time-variant channel impulse response from the transmitter to the receiver is denoted as $h(\tau,t)$ where it represents the response at time t with an impulse applied at time $t-\tau$, which indicates that in a general setup, the system is time-varying. The input-output relation for a SISO system is given by

$$r(t)=\int_0^{\tau_{total}} h(\tau,t)\,x(t-\tau)\,d\tau = h(\tau,t)*x(t) \tag{2.1}$$

where $x(t)$ is the transmitted signal and $r(t)$ denotes the received signal at time t. The upper limit of the integral τ_{total} is the duration of the impulse response. The operator $*$ denotes the convolution operation [2].

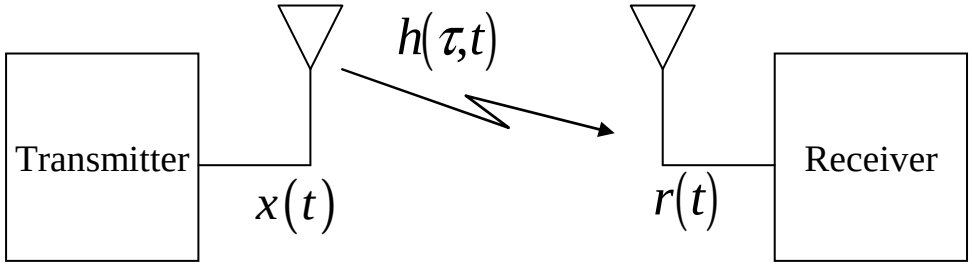

Figure 1. Schematic of a SISO System (After Ref. 2.)

2. Single-Input Multiple-Output (SIMO) Systems

A SIMO system has a single transmit antenna and multiple (M_r) receive antennas. Figure 2 illustrates the schematic of a SIMO system.

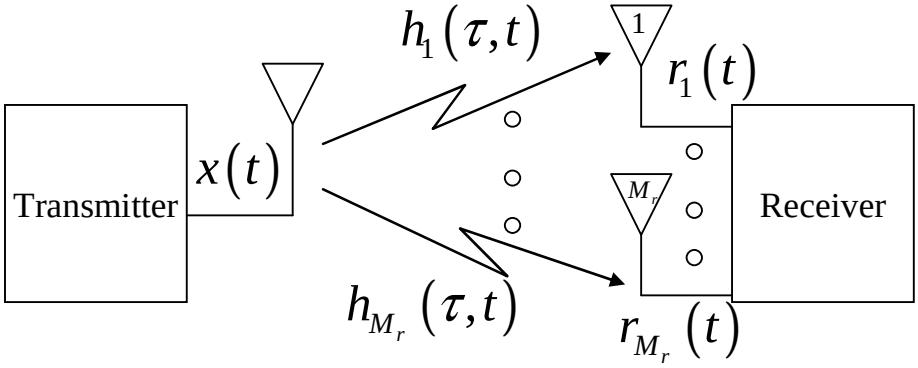

Figure 2. Schematic of a SIMO system (After Ref. 2.)

The channels $h_i(\tau,t),\ i=1,2,\ldots,M_r$, represent the impulse responses from the single transmit antenna to the M_r receive antennas. The received signals at the respective receive antennas are given by

$$\begin{aligned} r_1(t) &= h_1(\tau,t) * x(t) \\ r_2(t) &= h_2(\tau,t) * x(t) \\ &\vdots \\ r_{M_r}(t) &= h_{M_r}(\tau,t) * x(t). \end{aligned} \tag{2.2}$$

Representing the signals at the receiver antennas in a vector form, we have the received signal vector

$$\mathbf{r}(t) = \begin{bmatrix} r_1(t) & r_2(t) & \cdots & r_{M_r}(t) \end{bmatrix}^T. \tag{2.3}$$

Similarly, the channel vector is given by

$$\mathbf{h}(t) = \begin{bmatrix} h_1(t) & h_2(t) & \cdots & h_{M_r}(t) \end{bmatrix}^T. \tag{2.4}$$

Therefore, we can express the input-output relationship of a SIMO system as

$$\mathbf{r}(t) = \mathbf{h}(\tau,t) \star x(t) \tag{2.5}$$

where the operator $\star$ denotes the element-by-element convolution.

3. Multiple-Input Single-Output (MISO) Systems

Figure 3 depicts a simple MISO system with multiple (M_t) transmit antennas and a single receive antenna. Input-output relationship of a MISO system can be developed on the lines of a SIMO system as discussed above. The multiple transmitted signals $x_j(\tau,t),\ \ j=1,2,\ldots,M_t$, are convolved with the channel impulse responses $h_j(\tau,t),\ \ j=1,2,\ldots,M_t$. The receiving antenna receives a superposition of the multian-tenna transmissions through the channels [12]. Accordingly, the received signal can be expressed as

$$r(t)=x_1(t)*h_1(\tau,t)+x_2(t)*h_2(\tau,t)+\ldots+x_{M_t}(t)*h_{M_t}(\tau,t)\ . \tag{2.6}$$

Using the vector notation for the received signal equation (2.6), we can write the input-output relation for a MISO system as

$$r(t)=\mathbf{h}(\tau,t)\star\mathbf{x}(t) \tag{2.7}$$

where $\mathbf{x}(t)=\begin{bmatrix}x_1(t) & x_2(t) & \cdots & x_{M_t}(t)\end{bmatrix}^T$ is the transmission vector, and the channel vector is denoted as $\mathbf{h}(t)=\begin{bmatrix}h_1(t) & h_2(t) & \cdots & h_{M_t}(t)\end{bmatrix}$.

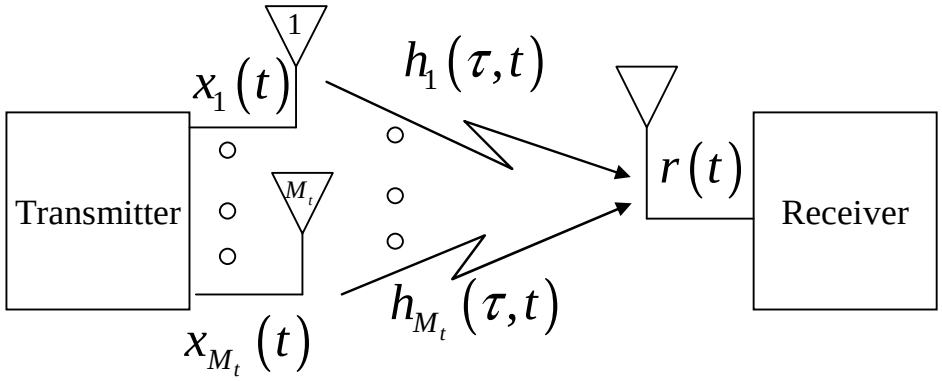

Figure 3. Schematic of a MISO System (After Ref. 2.)

4. Multiple-Input Multiple-Output (MIMO) Systems

After discussing the input-output relations for the SIMO and the MISO systems, we now proceed to develop the MIMO system relations. A simple MIMO system is illus-trated in Figure 4. The received signal at the first receive antenna is expressed by

$$r_1(t) = x_1(t) * h_{1,1}(\tau,t) + \ldots + x_{M_t}(t) * h_{1,M_t}(\tau,t) \ . \tag{2.8}$$

This is analogous to the MISO system input-output relation. The received signal at the M_r-th receive antenna is given by

$$r_{M_r}(t) = x_1(t) * h_{M_r,1}(\tau,t) + \ldots + x_{M_t}(t) * h_{M_r,M_t}(\tau,t) \ . \tag{2.9}$$

The general input-output relation for a MIMO system in matrix-vector notation is given by

$$\mathbf{r}(t) = \mathbf{H}(\tau,t) \bigstar \mathbf{x}(t) \tag{2.10}$$

where $\mathbf{x}(t) = \begin{bmatrix} x_1(t) & x_2(t) & \cdots & x_{M_t}(t) \end{bmatrix}^T$ is the $M_t \times 1$ transmission vector, $\mathbf{r}(t) = \begin{bmatrix} r_1(t) & r_2(t) & \cdots & r_{M_t}(t) \end{bmatrix}^T$ is the $M_r \times 1$ receive vector, and $\mathbf{H}(\tau,t)$ is the $M_r \times M_t$ channel matrix given by

$$\mathbf{H}(\tau,t) = \begin{bmatrix} h_{1,1}(\tau,t) & h_{2,2}(\tau,t) & \cdots & h_{1,M_t}(\tau,t) \\ h_{2,1}(\tau,t) & h_{2,2}(\tau,t) & \cdots & h_{2,M_t}(\tau,t) \\ \vdots & \vdots & \ddots & \vdots \\ h_{M_r,1}(\tau,t) & h_{M_r,2}(\tau,t) & \ldots & h_{M_r,M_t}(\tau,t) \end{bmatrix}. \tag{2.11}$$

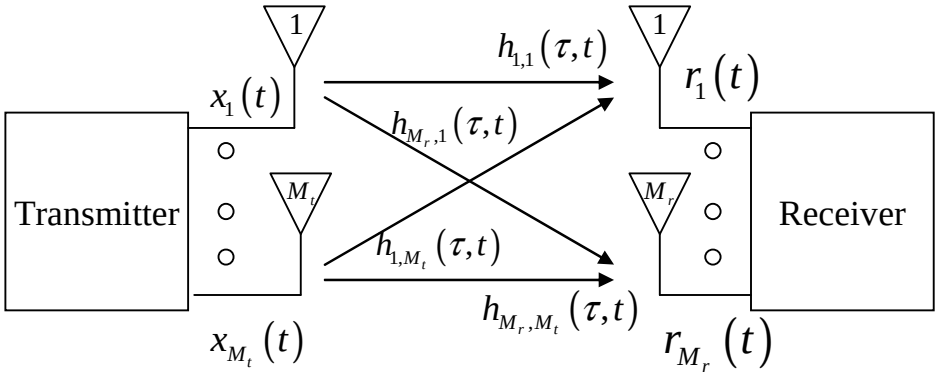

Figure 4. Schematic of a MIMO System (After Ref. 2.)

B. ALAMOUTI SCHEME

The Alamouti transmit diversity technique was proposed in 1998 [4]. The technique is generally referred to as the Alamouti scheme in the literature. Alamouti scheme is one of the first space coding schemes developed for the MIMO systems. Since the scheme has a simple transmit coding technique and a simple decoding implementation, it gained considerable interest.

The Alamouti scheme was developed for systems under flat fading conditions, i.e., over frequency independent channels. Therefore, while discussing the scheme, the indices of delay τ and time t of the channels are dropped. The channels are denoted as $h_i, i = 1, 2$, representing single-tap impulse responses. Prior to developing the Alamouti scheme, we first need to present the input-output relations of the SIMO system using a maximal ratio combining scheme.

1. Maximal Ratio Combining (MRC) Scheme for 1×2 Systems

Maximal ratio combining (MRC) scheme is developed for the systems having multiple receive antennas, i.e., multiple channels. The scheme is based on the assumption that the receiver has perfect channel knowledge. The transmitted information is estimated by processing the channel state information (CSI) and the received signals [5]. The channel information may be obtained by inserting known pilot symbols. The receiver estimates the channel information by interpolating the samples of the received pilot symbols [4].

Figure 5 illustrates a 1×2 system employing MRC. The impulse response of the channel from the transmit antenna to the receive antenna 1 is denoted by h_1 and to the receive antenna 2 is denoted by h_2. Assuming that the channels have flat fading, received signals with additive noise are expressed by

$$\begin{aligned} r_1 &= h_1 s_1 + n_1 \\ r_2 &= h_2 s_1 + n_2 \end{aligned} \tag{2.12}$$

where s_1 is the transmitted information symbol and n_1 and n_2 denote the complex noise components. The MRC uses the CSI and the received signals r_1 and r_2 to compute the estimated value of s_1. The MRC obtains an estimate of s_1 using the relation [4]

$$\tilde{s}_1 = h_1^* r_1 + h_2^* r_2 . \tag{2.13}$$

The combining scheme compensates for the phase shift in the channel by multiplying the received signal with the complex-conjugate of the corresponding channel [5]. Substituting (2.12) into (2.13), we can rewrite the estimate of s_1 as

$$\tilde{s}_1 = \left(|h_1|^2 + |h_2|^2 \right) s_1 + h_1^* n_1 + h_2^* n_2 . \tag{2.14}$$

The constructed complex value $\tilde{s}_1$ is the maximum likelihood estimate of the transmitted symbol [4]. The estimate of the transmitted symbol is mostly dependent upon the magnitudes of the channels h_1 and h_2, i.e., MRC is resistant to phase changes of the channels.

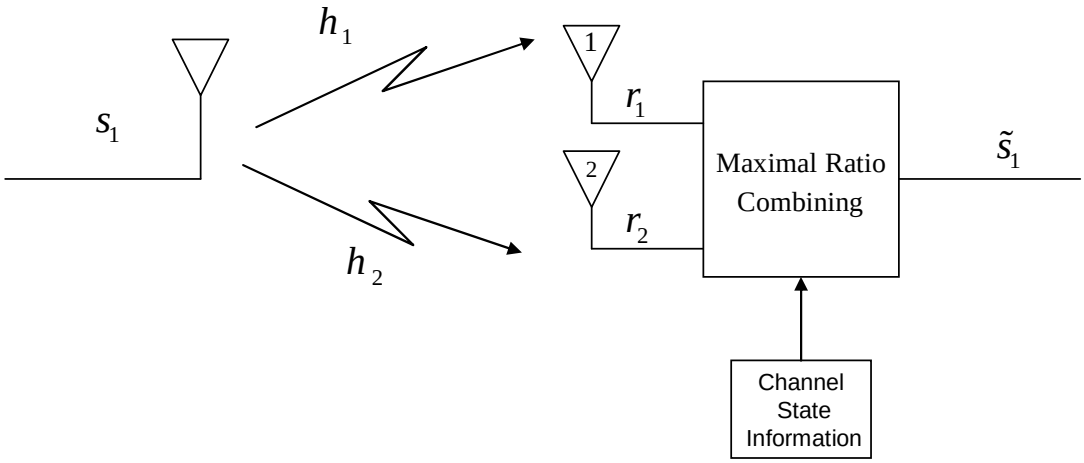

Figure 5. Maximal Ratio Combining for a 1×2 System (After Ref. 4.)

2. Alamouti Scheme for 2×1 Systems

The Alamouti scheme for a system with two transmit antennas and a single receive antenna is shown in Figure 6. Two consecutive symbols s_1 and s_2 are transmitted simultaneously during the first symbol period (at time = t). During the next symbol period (at time = $t + T$), $-s_2^*$ and s_1^* are transmitted from antenna 1 and 2, respectively, where the asterisk $*$ indicates complex conjugation. The transmission sequence is shown in Table 1.

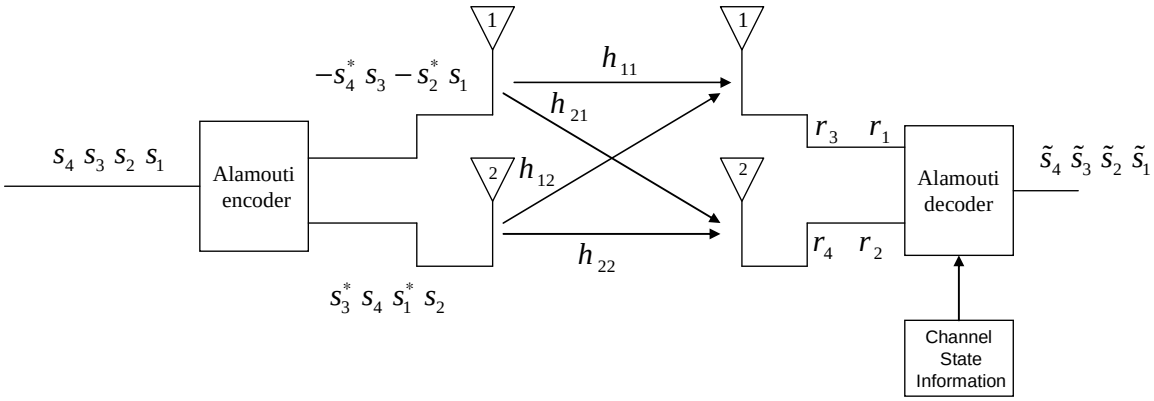

Figure 6. Alamouti Scheme for a 2×2 System (After Ref. 4.)

Time	Transmit Antenna-1	Transmit Antenna-2
t	s_1	s_2
$t+T$	$-s_2^*$	s_1^*

Table 1. Transmission Sequence of the Alamouti Scheme

The received signal at time *t*, which is the superposition of the two incoming signals, can be expressed by

$$r_1 = r(t) = h_1 s_1 + h_2 s_2 + n_1 \tag{2.15}$$

where n_1 is the additive complex noise component. Assuming that the channel is constant across two consecutive symbol periods, we can express the received signal at time $t+T$ as

$$r_2 = r(t+T) = h_2 s_1^* - h_1 s_2^* + n_2 \tag{2.16}$$

where n_2 is the additive complex noise component.

Two consecutive received signals and the CSI are employed at the Alamouti decoder. The estimates of the transmitted symbols are computed by [4]

$$\begin{aligned} \tilde{s}_1 &= h_1^* r_1 + h_2 r_2^* \\ \tilde{s}_2 &= h_2^* r_1 - h_1 r_2^*. \end{aligned} \tag{2.17}$$

Substituting (2.15) and (2.16) into (2.17), we can rewrite the decoder equations as

$$\begin{aligned} \tilde{s}_1 &= \left(|h_1|^2 + |h_2|^2\right) s_1 + h_1^* n_1 + h_2 n_2^* \\ \tilde{s}_2 &= \left(|h_1|^2 + |h_2|^2\right) s_2 + h_2^* n_1 - h_1 n_2^*. \end{aligned} \tag{2.18}$$

This outcome shows that the Alamouti decoder compensates the phase changes of the channel in a manner similar to that in the MRC scheme.

3. Alamouti Scheme for 2×2 Systems

We can extend the 2×1 Alamouti scheme to a 2×2 system by adding one more receiving antenna. A schematic of the Alamouti scheme for a 2×2 system is illustrated in Figure 7. The transmission sequence is identical to the one in the 2×1 system (see Table 1), but the decoding scheme will be different.

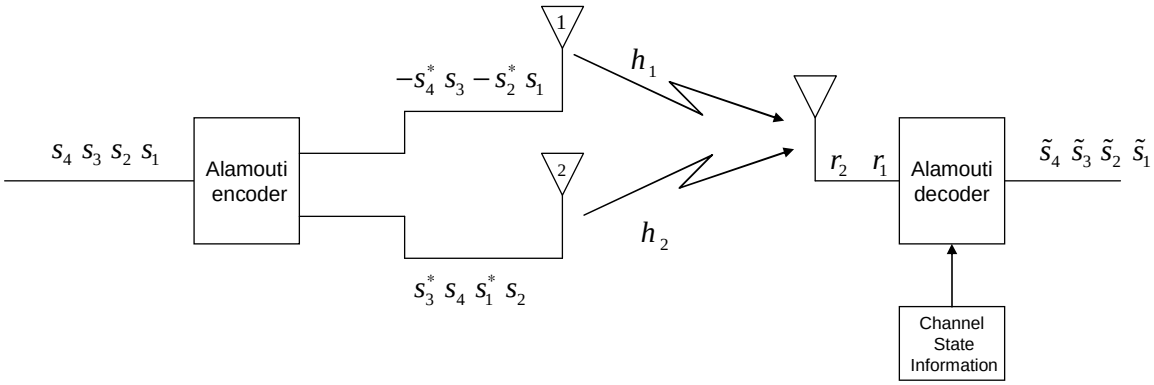

Figure 7. Alamouti Scheme for a 2×1 System (After Ref. 4.)

Assuming that the channel is constant across consecutive symbol periods, the received signals can be expressed by

$$\begin{aligned} r_1 &= h_{1,1}s_1 + h_{1,2}s_2 + n_1 \\ r_2 &= h_{2,1}s_1 + h_{2,2}s_2 + n_2 \\ r_3 &= -h_{1,1}s_2^* + h_{1,2}s_1^* + n_3 \\ r_4 &= -h_{2,1}s_2^* + h_{2,2}s_1^* + n_4 \end{aligned} \tag{2.19}$$

where $n_i,\ \ i = 1,2,3,4$, are the complex noise components. Table 2 lists the notation for the received signals at the receive antennas. The channel impulse responses $h_{i,j},\ \ i, j = 1,2$, represent the four possible paths in the scheme.

Time	**Receive Antenna-1**	**Receive Antenna-2**
t	r_1	r_2
$t+T$	r_3	r_4

Table 2. Notation for the Received Signals in 2×2 Alamouti Scheme

The Alamouti decoder constructs the estimates of s_1 and s_2 using the CSI, the received signals and the decoding equations given by [4]

$$\begin{aligned}\tilde{s}_1 &= h_{1,1}^* r_1 + h_{1,2} r_3^* + h_{2,1}^* r_2 + h_{2,2} r_4^* \\ \tilde{s}_2 &= h_{1,2}^* r_1 - h_{1,1} r_3^* + h_{2,2}^* r_2 - h_{2,1} r_4^*.\end{aligned} \tag{2.20}$$

Substituting (2.19) into (2.20), we can rewrite the decoder equations as

$$\begin{aligned}\tilde{s}_1 &= \left(|h_{1,1}|^2 + |h_{1,2}|^2 + |h_{2,1}|^2 + |h_{2,2}|^2\right) s_1 + h_{1,1}^* n_1 + h_{1,2} n_3^* + h_{2,1}^* n_2 + h_{2,2} n_4^* \\ \tilde{s}_2 &= \left(|h_{1,1}|^2 + |h_{1,2}|^2 + |h_{2,1}|^2 + |h_{2,2}|^2\right) s_2 + h_{1,2}^* n_1 - h_{1,1} n_3^* + h_{2,2}^* n_2 - h_{2,1} n_4^*.\end{aligned} \tag{2.21}$$

Clearly, we can see that the estimates mostly depend on the magnitudes of the channels so that the scheme is resistant to phase changes.

C. SUMMARY

This chapter discussed the input-output relations in MIMO systems, the MRC scheme for 2×1 systems and the Alamouti scheme for 2×1 and 2×2 systems. In all cases, only flat channel models are used to introduce the decoding process. In the next chapter, MIMO channel models for the frequency selective cases are introduced.

THIS PAGE INTENTIONALLY LEFT BLANK

III. MIMO CHANNEL MODELS

Building a channel model is important for investigating the performance of wireless communication systems. Channel parameters are extracted from measurements including path loss, Ricean *K*-factor, delay spread and Doppler spread for SISO systems and spatial correlation for MIMO systems. The Stanford University Interim (SUI) channels are widely used channel models based on such measurements. In the literature, most simulations, especially the IEEE 802.16a standard-based OFDM system simulations, are conducted using the SUI channel models. Generation of the SUI channels for SISO systems and the spatial correlation effects on correlated MIMO channels are discussed in this chapter.

A. STANFORD UNIVERSITY INTERIM (SUI) CHANNELS FOR THE IEEE 802.16a STANDARD

The IEEE 802.16 Broadband Wireless Access Working Group proposed channel models for fixed broadband systems in the year 2001. These channel models are known as Stanford University Interim (SUI) channel models because of the contribution of the Stanford University in the development process. The detailed channel generation is described in [11].

Three different terrain categories are defined in the SUI channel models. The maximum path loss category is hilly terrain with moderate-to-heavy tree densities (Category A). The minimum path loss category is typically flat terrain with light tree densities (Category C). The intermediate path loss category is Category B. The SUI channel models define two models for each terrain type, thus leading up to a total of six categories. Each channel model is characterized by a time delay, a Ricean *K*-factor and a Doppler spread in addition to the path loss behavior. The broad parameterization of the SUI channels is summarized in Table 3. From this classification, we can easily see that the SUI-1 channel is the least severe channel model with a low delay spread ($0.4\ \mu$s for the 2nd tap and $0.9\ \mu$s for the 3rd tap), a low Doppler spread (0.4 Hz, 0.3 Hz, 0.5 Hz for the 1st, 2nd and 3rd taps, respectively) and a high *K*-factor (8 dB for the 1st tap). The most severe channel is certainly the SUI-6 model with a high delay spread ($4\ \mu$s for the 2nd tap and

10 μs for the 3rd tap), a high Doppler spread (2 Hz, 1.5 Hz, 2.5 Hz, for the 1st, 2nd and 3rd taps, respectively) and $K = 0$, i.e., no direct path component but only a fading component (see Appendix A for details of all SUI model parameters).

SUI-Model	**Terrain Type**	**Delay Spread**	**Ricean *K* Factor**	**Doppler**
SUI-1	C	Low	High	Low
SUI-2	C	Low	High	Low
SUI-3	B	Low	Low	Low
SUI-4	B	Moderate	Low	High
SUI-5	A	High	Low	Low
SUI-6	A	High	Low	High

Table 3. SUI Channel Characterization (After Ref. 13.)

Each of the six SUI channels is modeled as a 3-tap discrete system with non-uniform delays, i.e., multipath fading exists for each SUI model. The SUI channels are also modeled for different antenna types. Each channel has parameters defined for an omni-directional antenna and for a 30° directional antenna. The detailed parameters for the omni-directional and for the 30° directional antenna case are given in Appendix A.

The latest IEEE 802.16 Broadband Wireless Access Working Group report [11] contains a complimentary Matlab code for generating channels for the SUI-3 model. In this thesis, to create a simulation environment, an expanded version of Matlab code (containing all six SUI channels) was developed based on the code in [11].

After generating the SUI channel model in Matlab, the frequency responses of the channel models were investigated. The frequency response plots of five different SUI channels are shown in Figure 8. The frequency range was chosen to be in terms of the subcarrier index 0-255 in accordance with the fast Fourier transform (FFT) size of the IEEE 802.16a standard. The frequency response was normalized such that the maximum magnitude was 1. By observing the fluctuations of the magnitude values, the SUI-1

channel's magnitude response changes smoothly between 0.9 and 1.0 where as the SUI-5 channel's magnitude response varies rapidly between 0.5 and 1.0. As a result, the higher the SUI channel index, the more frequency selective is the channel.

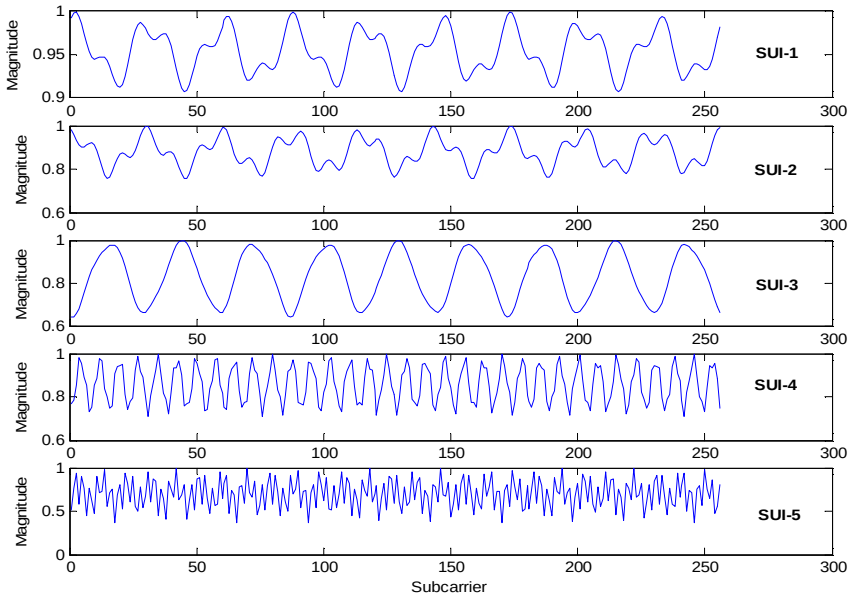

Figure 8. The Frequency Response Plots of Different SUI Channel Models

B. GENERATING CORRELATED MIMO CHANNELS

Since there are multiple antennas at both ends of MIMO systems, the presence of spatial correlation has an effect on the channels. The ideal case is that all channels in a MIMO system are independent, i.e., uncorrelated with each other. In reality, however, the physical configuration of the antennas (antenna spacing) and operating environment parameters (angle of arrival and angle of departure of the electromagnetic waves) cause spatial correlation on the antenna array of a MIMO system. A MIMO system's performance is reduced by this spatial correlation. An analysis of spatial correlation is discussed in [14].

1. Uncorrelated MIMO Channels

Consider a system with M_t transmit and M_r receive antennas. Assuming that all the channels are flat and uncorrelated (i.e., each path is represented by a single complex tap weight), the MIMO channel can be modeled to be zero mean and circularly symmet-

ric with unit variance. The uncorrelated channel is an identically and independently distributed channel, denoted as $\mathbf{H}_w$ with dimensions $M_r \times M_t$. The properties of $\mathbf{H}_w$ are

$$\begin{aligned} E\left\{\left|\mathbf{H}_{w_{i,j}}\right|\right\} &= 0 \\ E\left\{\left|\mathbf{H}_{w_{i,j}}\right|^2\right\} &= 1 \\ E\left\{\left|\mathbf{H}_{w_{i,j}}\right|\left|\mathbf{H}_{w_{m,n}}\right|\right\} &= 0 \quad \text{if } i \neq m \text{ or } j \neq n \end{aligned} \tag{3.1}$$

where $E\{\bullet\}$ denotes the expectation operator [2].

2. Correlated MIMO Channels

In practice, MIMO channels can differ from $\mathbf{H}_w$ because of the spatial correlation. A more practical MIMO channel can be expressed as [2]

$$\mathbf{H} = \mathbf{R}_r^{1/2}\mathbf{H}_w\mathbf{R}_t^{1/2} \tag{3.2}$$

where $\mathbf{R}_r$ is the $M_r \times M_r$ receive correlation matrix and $\mathbf{R}_t$ is the $M_t \times M_t$ transmit correlation matrix. The correlation matrices $\mathbf{R}_r$ and $\mathbf{R}_t$ are positive semi-definite Hermitian matrices and have the following properties:

$$\begin{aligned} \mathbf{R}_r &= \mathbf{R}_r^{1/2}\mathbf{R}_r^{1/2} \\ \mathbf{R}_t &= \mathbf{R}_t^{1/2}\mathbf{R}_t^{1/2}. \end{aligned} \tag{3.3}$$

The correlation matrices for a 2×2 system can be generated in the following form [11]:

$$\mathbf{R}_r = \begin{bmatrix} 1 & \rho_r \\ \rho_r & 1 \end{bmatrix}, \tag{3.4}$$

$$\mathbf{R}_t = \begin{bmatrix} 1 & \rho_t \\ \rho_t & 1 \end{bmatrix} \tag{3.5}$$

where ρ_r and ρ_t denote the receive and transmit correlation coefficients. The spatial fading coefficient is dependent upon the distance between the antennas, the wavelength and the geometry of the physical environment and takes values between 0 and 1. When the transmit and receive correlation coefficients are both equal to zero, the correlation matrices $\mathbf{R}_r$ and $\mathbf{R}_t$ become identity matrices, and then the MIMO channel will be equal to the uncorrelated channel $\mathbf{H}_w$. The computation of the correlation coefficients is presented in

detail in [14]. In this thesis, the environmental parameters (antenna spacing, angle of arrival and angle of departure of the electromagnetic waves) were not taken into account to compute the correlation coefficients. The correlation coefficient parameters were chosen arbitrarily.

3. LOS Component

In the presence of a line-of-sight (LOS) component, MIMO channels have a fixed and a random component. The MIMO channel with a LOS component can be represented as [2]

$$\mathbf{H} = \sqrt{\frac{K}{1+K}}\bar{\mathbf{H}} + \sqrt{\frac{1}{1+K}}\mathbf{H}_w \tag{3.6}$$

where $\sqrt{K/(1+K)}\bar{\mathbf{H}}$ is the LOS and $\sqrt{1/(1+K)}\mathbf{H}_w$ is the random uncorrelated fading component. The elements of $\bar{\mathbf{H}}$ have unit power. The Ricean *K*-factor in (3.6) is the ratio of the LOS component power to the fading component power. When $K = 0$, the channel becomes pure Rayleigh faded channel, i.e., there is no LOS component. When $K = \infty$, all we have is the LOS component, and there is no fading component. Then the channel becomes flat [2].

In the presence of both spatial correlation and LOS component, to achieve a complete MIMO channel, only the fading component is computed using (3.2), and the fixed LOS component is added to the fading component using (3.6).

The generation of the correlated SIMO and MISO channels are similar to the MIMO channels. Consider a system with a single transmit and two receive antennas. The uncorrelated SIMO channel $\mathbf{H}_w$ is a 2×1 row vector. Since we have a single transmit antenna, there is no transmit correlation, i.e., $\rho_t = 0$. The transmit covariance matrix $\mathbf{R}_t$ is then an identity matrix. From (3.2), the correlated SIMO channel can be expressed as

$$\mathbf{H} = \mathbf{R}_r^{1/2}\mathbf{H}_w \tag{3.7}$$

where $\mathbf{R}_r^{1/2}$ is the square-root of the receive correlation matrix $\mathbf{R}_r$.

For the MISO case, consider a system with two transmit antennas and a single receive antenna. The uncorrelated MISO channel $\mathbf{H}_w$ will be a 1×2 column vector. Since

there are multiple antennas only at the transmitter, the receive correlation matrix $\mathbf{R}_r$ is an identity matrix. The correlated MISO channel is expressed by

$$\mathbf{H} = \mathbf{H}_w \mathbf{R}_t^{1/2} \tag{3.8}$$

where $\mathbf{R}_t^{1/2}$ is the square-root of the transmit correlation matrix $\mathbf{R}_t$.

In the presence of a LOS component, the fixed components of the MISO and the SIMO channel are added to the correlated fading components of the MISO and the SIMO channels, respectively. The complete MISO or SIMO channel is achieved by the relation given in (3.6).

C. GENERATING CORRELATED FREQUENCY-SELECTIVE MIMO CHANNELS

The generation of the SUI channels for SISO systems and correlated flat MIMO channels have been discussed so far. The uncorrelated channel $\mathbf{H}_w$ in (3.2) has single-tap complex components for the flat channel case. The frequency selective channels have multi-tap components. To study the correlated frequency selective MIMO channels, consider a system with two transmit and two receive antennas operating over the MIMO channels generated by the SUI models. Each tap is characterized by a delay spread, a power level, a Doppler spread and a Ricean *K*-factor. Therefore, a SUI channel has a fixed and a fading component for each tap. The fading component includes the delay spread, the Doppler spread and the power level. The fixed component is generated with the specified Ricean *K*-factor for the given SUI model [11]. In a MIMO channel for a 2×2 system based on SUI channel modeling, the fading and fixed components can be expressed as

$$\mathbf{H}_w = \begin{bmatrix} h_{11}(1) & h_{11}(2) & h_{11}(3) & h_{12}(1) & h_{12}(2) & h_{12}(3) \\ h_{21}(1) & h_{21}(2) & h_{21}(3) & h_{22}(1) & h_{22}(2) & h_{22}(3) \end{bmatrix} \tag{3.9}$$

$$\bar{\mathbf{H}} = \begin{bmatrix} \bar{h}_{11}(1) & \bar{h}_{11}(2) & \bar{h}_{11}(3) & \bar{h}_{12}(1) & \bar{h}_{12}(2) & \bar{h}_{12}(3) \\ \bar{h}_{21}(1) & \bar{h}_{21}(2) & \bar{h}_{21}(3) & \bar{h}_{22}(1) & \bar{h}_{22}(2) & \bar{h}_{22}(3) \end{bmatrix}, \tag{3.10}$$

respectively, where $h_{ij}(k)$ is the channel response between the i-th$(i=1,2)$ transmit antenna and the j-th $(j=1,2)$ receive antenna for the k-th$(k=1,2,3)$ tap. Assuming that all

tap correlations are equal, the correlated fading component of the MIMO channel is expressed by

$$\hat{\mathbf{H}}_{ij}(k) = \mathbf{R}_r^{1/2} \mathbf{H}_{w_{ij}}(k) \mathbf{R}_t^{1/2} \tag{3.11}$$

where $\mathbf{H}_{w_{ij}}(k)$ is the 2×2 uncorrelated channel matrix for the *k*-th tap.

To achieve the complete MIMO channel, the LOS component will be added to the correlated fading component. Then the MIMO channel is given by

$$\mathbf{H}_{ij}(k) = \sqrt{\frac{K}{1+K}} \bar{\mathbf{H}}_{ij}(k) + \sqrt{\frac{1}{1+K}} \hat{\mathbf{H}}_{ij}(k) \tag{3.12}$$

where $\bar{\mathbf{H}}_{ij}(k)$ is the fixed component between the *i*-th $(i = 1, 2)$ transmit antenna and the *j*-th $(j = 1, 2)$ receive antenna for the *k*-th $(k = 1, 2, 3)$ tap. Generation of a correlated MIMO channel is illustrated in Figure 9.

D. SUMMARY

In this chapter, the generation of SUI channels for SISO systems, uncorrelated MIMO channels and spatial correlation effects on flat and frequency selective MIMO channels were discussed. It was demonstrated that the channel becomes more frequency selective as the SUI index increases.

In the next chapter, we will develop the input-output relations for the Alamouti scheme based STBC systems over frequency selective multi-tap channels.

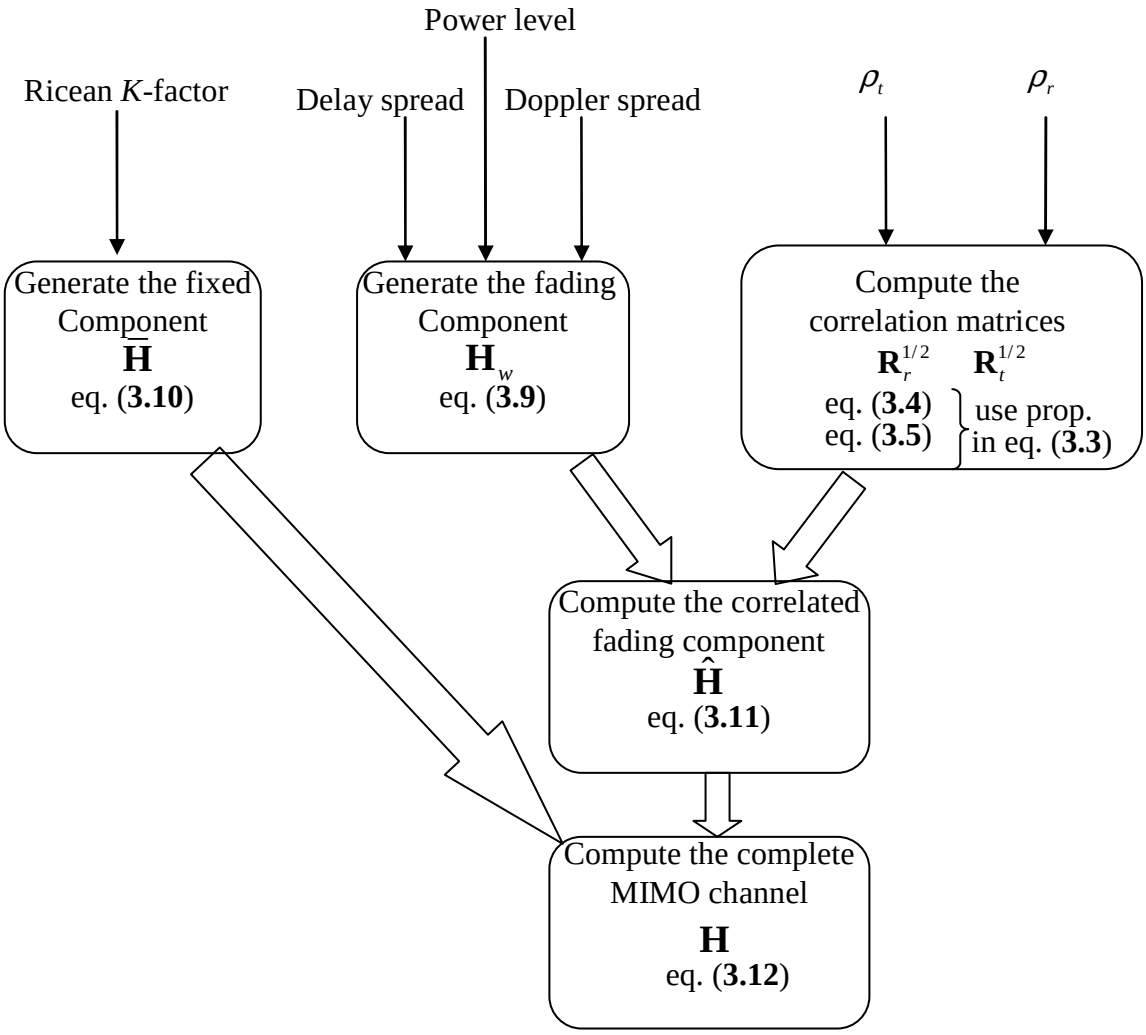

Figure 9. Conceptual Diagram for Generating a Correlated MIMO Channel Based on SUI Channel Models

IV. ALAMOUTI-BASED SCHEMES OVER FREQUENCY-SELECTIVE CHANNELS

The transmitted signals experience different types of fading depending upon the relationship between the signal parameters (bandwidth, symbol period, etc.) and the channel parameters (Doppler spread, delay spread, etc.). When the bandwidth of the channel is greater than the bandwidth of the transmitted signal, the received signal experiences a flat fading channel. A flat channel is approximated as a single-tap weight with zero delay. When the bandwidth of the channel is greater than the bandwidth of the transmitted signal, the received signal experiences a frequency selective channel or a multipath fading channel. Over frequency selective channels, multiple versions of the transmitted signal having faded amplitudes arrive at the receiver at slightly different time instants. Frequency selective channels are modeled by multiple tap discrete systems with different delay parameters [15].

Alamouti's transmit diversity scheme, which was discussed in Chapter II, was originally proposed for flat channels. The space coding technique is performed over a symbol pair, i.e., two consecutive symbols (see Table 1). The decoding equations (2.17) and (2.20) are developed for flat channels. The frequency-flat channels in these equations are represented as one-tap complex weights. The extension of the Alamouti scheme to frequency-selective channels was investigated in [8] and [9]. The extended scheme is called space-time block coding (STBC), since space coding is performed over blocks of symbols. The scheme presented in [8] and [9] is for the systems with two transmit antennas and a single receive antenna (2×1). In this thesis, the scheme is further extended to 1×2 and 2×2 systems using the original Alamouti scheme.

OFDM has emerged as an attractive alternative scheme to conventional modulation schemes due to its effectiveness in reducing the effects of frequency selective channels [7]. The combination of MIMO systems and OFDM modulation is one of the widely discussed areas in the MIMO research. Different space coding techniques in MIMO-OFDM systems have been investigated by many authors [6, 7, 16]. In this work, we have selected the STBC scheme as the space coding scheme for MIMO-OFDM systems to

study its simulation performance and compare its performance to that of STBC-SC systems. The STBC scheme is chosen as an optional technique in the OFDM physical layer specifications of the IEEE 802.16a standard.

In this chapter, we discuss the STBC coding technique for the MIMO systems with both single-carrier modulation and OFDM. Input-output relations and the decoding equations are presented for SISO, SIMO, MISO and MIMO systems.

A. SPACE-TIME BLOCK CODING-SINGLE CARRIER (STBC-SC) SYSTEMS OVER FREQUENCY-SELECTIVE CHANNELS

Before discussing the STBC schemes, in order to get familiar with the notation, the discrete-time SISO system relations over frequency selective channels are introduced first.

1. SISO Systems over Frequency-Selective Channels

Consider that a block of symbols is transmitted from a single antenna by assuming that the channel characteristics do not change during the period of transmission. The transmitted block of symbols is expressed by

$$\mathbf{S} = \begin{bmatrix} s(1) & s(2) & \dots & s(N) \end{bmatrix} \tag{4.1}$$

where N is the block size. The transmitted symbol block will experience a frequency selective channel. The channel can be represented as a discrete-time filter given by

$$h\left(q^{-1}\right) = h_0 + h_1 q^{-1} + \dots h_P q^{-P} \tag{4.2}$$

where q^{-1} is the unit delay operator and $h_n, n = 1, 2, \dots P$ are the filter coefficients. The received signal can be expressed as

$$r(t) = h\left(q^{-1}\right) s(t) = h_0 s(t) + h_1 s(t-1) + \dots h_P s(t-P). \tag{4.3}$$

The noise component of the received signal is omitted here for convenience. The maximum likelihood estimate of the transmitted symbols block is computed by

$$\tilde{s}(t) = h^*(q) r(t) = h_0^* r(t) + h_1^* r(t+1) + \dots + h_P^* r(t+P) \tag{4.4}$$

where $h^*(q)$ represents a non-causal realization of the filter given in (4.2) [8].

2. SIMO Systems over Frequency-Selective Channels

The schematic of a SIMO system over frequency selective channels is illustrated in Figure 10 for a 1×2 realization. The transmitted block of symbols is identical to the

SISO case (see Eq. (4.1)). Since there are two receive antennas, we have two channel filters given by

$$\begin{aligned} h_1\left(q^{-1}\right) &= h_{1_0} + h_{1_1} q^{-1} + \ldots + h_{1_P} q^{-P} \\ h_2\left(q^{-1}\right) &= h_{2_0} + h_{2_1} q^{-1} + \ldots + h_{2_P} q^{-P}. \end{aligned} \tag{4.5}$$

The transmitted signal is passed through these two channel filters, and the received signals are expressed by

$$\begin{aligned} r_1(t) &= h_1\left(q^{-1}\right) s(t) \\ r_2(t) &= h_2\left(q^{-1}\right) s(t). \end{aligned} \tag{4.6}$$

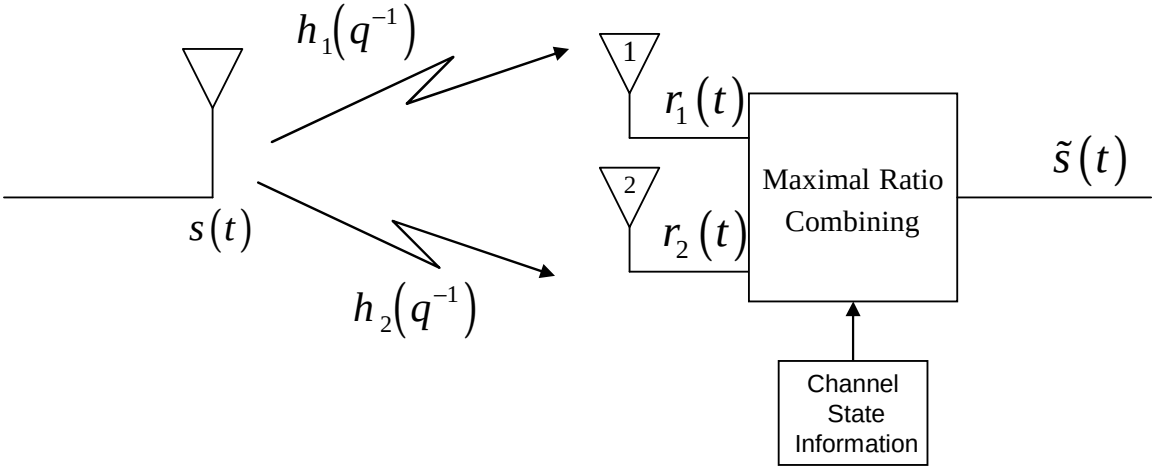

Figure 10. Schematic of a 1×2 SIMO-SC System Utilizing MRC over Frequency-Selective Channels

The estimate of the transmitted signal block is computed on the lines of the maximal ratio combining scheme. The multiplication operation in the decoding equation (2.13) is turned into a filter operation for the frequency selective channels. Accordingly, the estimate of the transmitted symbol block is given by [8]

$$s(t) = h_1^*(q)\, r_1(t) + h_2^*(q)\, r_2(t). \tag{4.7}$$

Notice that the conjugates of the filters $h_1^*(q)$ and $h_2^*(q)$ in (4.7) are non-casual filters. By substituting (4.5) into (4.7), the estimate of the transmitted signal block in (4.7) can be rewritten as

$$\begin{aligned} \tilde{s}(t) = {} & h_{1_0}^* r_1(t) + h_{1_1}^* r_1(t+1) + \ldots + h_{1_P}^* r_1(t+P) + h_{2_0}^* r_2(t) + \\ & h_{2_1}^* r_2(t+1) + \ldots + h_{2_P}^* r_2(t+P). \end{aligned} \tag{4.8}$$

3. MISO Systems over Frequency-Selective Channels

The Alamouti scheme for a 2×1 system over flat channels was discussed in Chapter II. The flat-channel implementation was based on applying the Alamouti encoding scheme over a symbol pair, i.e., two consecutive symbols. The scheme can be extended to the frequency-selective channel case by utilizing the STBC technique. A schematic of a 2×1 MISO system utilizing STBC is illustrated in Figure 11. The transmitted blocks of symbols are given by

$$\begin{aligned} \mathbf{S_1} &= \begin{bmatrix} s_1(1) & s_1(2) & \dots & s_1(N) \end{bmatrix} \\ \mathbf{S}_2 &= \begin{bmatrix} s_2(1) & s_2(2) & \dots & s_2(N) \end{bmatrix} \end{aligned} \tag{4.9}$$

where $\mathbf{S_1}$ and $\mathbf{S_2}$ are the simultaneously transmitted blocks of symbols from antenna 1 and antenna 2, respectively. The Alamouti space-time encoding scheme is performed over these two symbol blocks. The first antenna transmits a complex-conjugated and symbol-inverted version of $\mathbf{S_2}$, and the second antenna transmits a complex-conjugated version of $\mathbf{S_1}$ in the second transmission burst. The transmitted blocks of symbols in the second burst are given by

$$\begin{aligned} \mathbf{S_3} &= -\mathbf{S_2^*} = \begin{bmatrix} -s_1^*(1) & -s_1^*(2) & \dots & -s_1^*(N) \end{bmatrix} \\ \mathbf{S_4} &= \mathbf{S_1^*} = \begin{bmatrix} s_2^*(1) & s_2^*(2) & \dots & s_2^*(N) \end{bmatrix} \end{aligned} \tag{4.10}$$

where $\mathbf{S_3}$ and $\mathbf{S_4}$ are transmitted from antenna 1 and 2, respectively. The transmission symbol block sequence for the STBC for a 2×1 system is shown in Table 4.

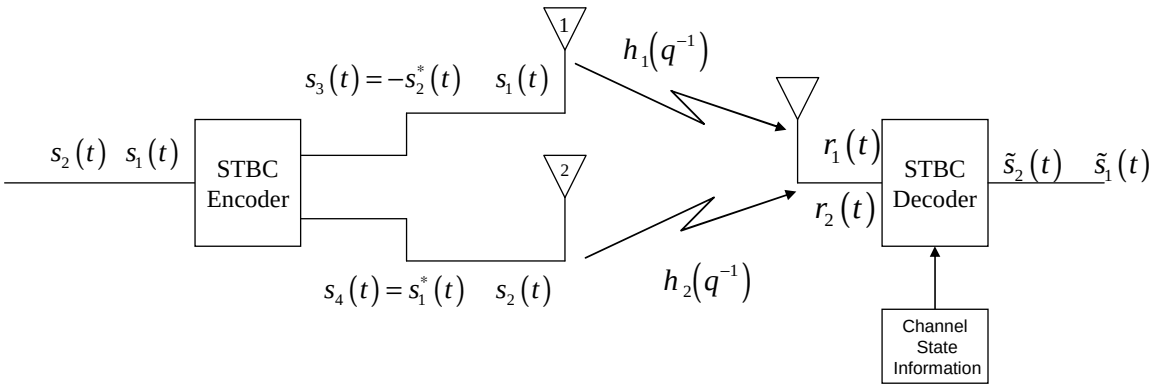

Figure 11. Schematic of a 2×1 STBC-SC System over Frequency-Selective Channels

Time	**Transmit Antenna-1**	**Transmit Antenna-2**
1st transmission burst	$\mathbf{S_1}$	$\mathbf{S_2}$
2nd transmission burst	$\mathbf{S_3} = -\mathbf{S_2^*}$	$\mathbf{S_4} = \mathbf{S_1^*}$

Table 4. Transmission Sequence for STBC

The notation of the channels for a 2×1 system is identical to the ones for the 1×2 system (see Eq. (4.5)). Assuming that the channel characteristics remain constant during consecutive transmissions of symbol blocks, the received signals are given by [8]

$$\begin{aligned} r_1(t) &= h_1\left(q^{-1}\right)s_1(t) + h_2\left(q^{-1}\right)s_2(t) \\ r_2(t) &= h_1\left(q^{-1}\right)s_3(t) + h_2\left(q^{-1}\right)s_4(t) \end{aligned} \tag{4.11}$$

where $r_1(t)$ and $r_2(t)$ denote the received signals during the 1st and 2nd transmission bursts, respectively. The 2×1 STBC decoder estimates the transmitted blocks of symbols using the decoding equations given by [4, 8]

$$\begin{aligned} \tilde{s}_1(t) &= h_1^*(q)\,r_1(t) + h_2\left(q^{-1}\right)r_2^*(t) \\ \tilde{s}_2(t) &= h_2^*(q)\,r_1(t) - h_1\left(q^{-1}\right)r_2^*(t) \end{aligned} \tag{4.12}$$

where $h_1^*(q)$ and $h_2^*(q)$ represent the non-causal realizations of the channel filters.

4. MIMO Systems over Frequency-Selective Channels

After discussing the SISO, SIMO and MISO systems over frequency-selective channels, we now proceed to develop the MIMO system relations. A schematic of a 2×2 MIMO system utilizing STBC is illustrated in Figure 12. The spatial encoding scheme is identical to the MISO system utilizing STBC. The transmitted blocks of symbols were introduced in Equations (4.9) and (4.10). The four MIMO channels for the 2×2 system are expressed as

$$
\begin{aligned}
h_{1,1}\left(q^{-1}\right) &= h_{1,1_0} + h_{1,1_1} q^{-1} + \ldots + h_{1,1_P} q^{-P} \\
h_{1,2}\left(q^{-1}\right) &= h_{1,2_0} + h_{1,2_1} q^{-1} + \ldots + h_{1,2_P} q^{-P} \\
h_{2,2}\left(q^{-1}\right) &= h_{2,2_0} + h_{2,2_1} q^{-1} + \ldots + h_{2,2_P} q^{-P} \\
h_{2,2}\left(q^{-1}\right) &= h_{2,2_0} + h_{2,2_1} q^{-1} + \ldots + h_{2,2_P} q^{-P}.
\end{aligned}
\tag{4.13}
$$

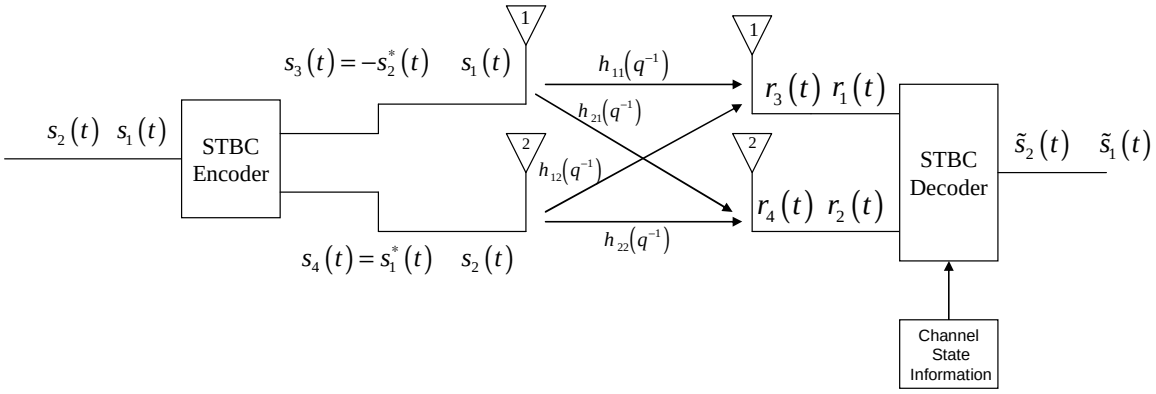

Figure 12. Schematic of a 2×2 STBC-SC System over Frequency-Selective Channels

Assuming that the channel characteristics remain constant over two transmission bursts, the received signals are given by

$$
\begin{aligned}
r_1(t) &= h_{1,1}\left(q^{-1}\right) s_1(t) + h_{1,2}\left(q^{-1}\right) s_2(t) \\
r_2(t) &= h_{2,1}\left(q^{-1}\right) s_1(t) + h_{2,2}\left(q^{-1}\right) s_2(t) \\
r_3(t) &= h_{1,1}\left(q^{-1}\right) s_3(t) + h_{1,2}\left(q^{-1}\right) s_4(t) \\
r_4(t) &= h_{2,1}\left(q^{-1}\right) s_3(t) + h_{2,2}\left(q^{-1}\right) s_4(t).
\end{aligned}
\tag{4.14}
$$

The sequence and the location of the received symbol blocks in (4.14) are given in Table 5. The STBC decoder estimates the transmitted blocks of symbols by using the decoding equations [4, 8]

$$
\begin{aligned}
\tilde{s}_1(t) &= h_{1,1}^*(q)\, r_1(t) + h_{1,2}\left(q^{-1}\right) r_3^*(t) + h_{2,1}^*(q) r_2(t) + h_{2,2}\left(q^{-1}\right) r_4^*(t) \\
\tilde{s}_2(t) &= h_{1,2}^*(q)\, r_1(t) - h_{1,1}\left(q^{-1}\right) r_3^*(t) + h_{2,2}^*(q)\, r_2(t) - h_{2,1}\left(q^{-1}\right) r_4^*(t).
\end{aligned}
\tag{4.15}
$$

where $h_{i,j}^*(q)$, $i = 1,2$; $j = 1,2$, represent the non-causal realizations of the channel filters. The equations in (4.15) are similar to the flat channel Alamouti decoding equations previously introduced in (2.20). The multiplication operation in the flat channel case is now replaced by the filter operation.

	Receive Antenna-1	**Receive Antenna-2**
1st transmission burst	$r_1(t)$	$r_2(t)$
2nd transmission burst	$r_3(t)$	$r_4(t)$

Table 5. The Sequence and the Location of the Received Signals for a 2×2 STBC System

B. SPACE-TIME BLOCK CODING-ORTHOGONAL FREQUENCY DIVISION MULTIPLEXING (STBC-OFDM) SYSTEMS OVER FREQUENCY-SELECTIVE CHANNELS

In the previous section, we discussed the single-carrier MIMO systems utilizing STBC over frequency-selective channels. The combination of STBC and OFDM is discussed in this and the following sections. OFDM has emerged as an attractive and alternative scheme to the conventional modulation schemes due to its effectiveness in reducing the effects of frequency-selective channels [7]. In OFDM, the entire signal bandwidth is divided into a number of orthogonal subcarrier bands, and then the signal is transmitted in these narrowbands over a number of subcarriers. The OFDM and STBC parameters were selected from the IEEE 802.16a standard [10]. The IEEE 802.16a standard includes the 2×1 STBC scheme as an optional specification for systems employing OFDM.

1. SISO-OFDM Systems over Frequency-Selective Channels

A block diagram of a SISO-OFDM system is shown in Figure 13. A detailed explanation of each block is given in the following discussion. The physical layer part of the IEEE 802.16a standard is used in describing the SISO-OFDM scheme here.

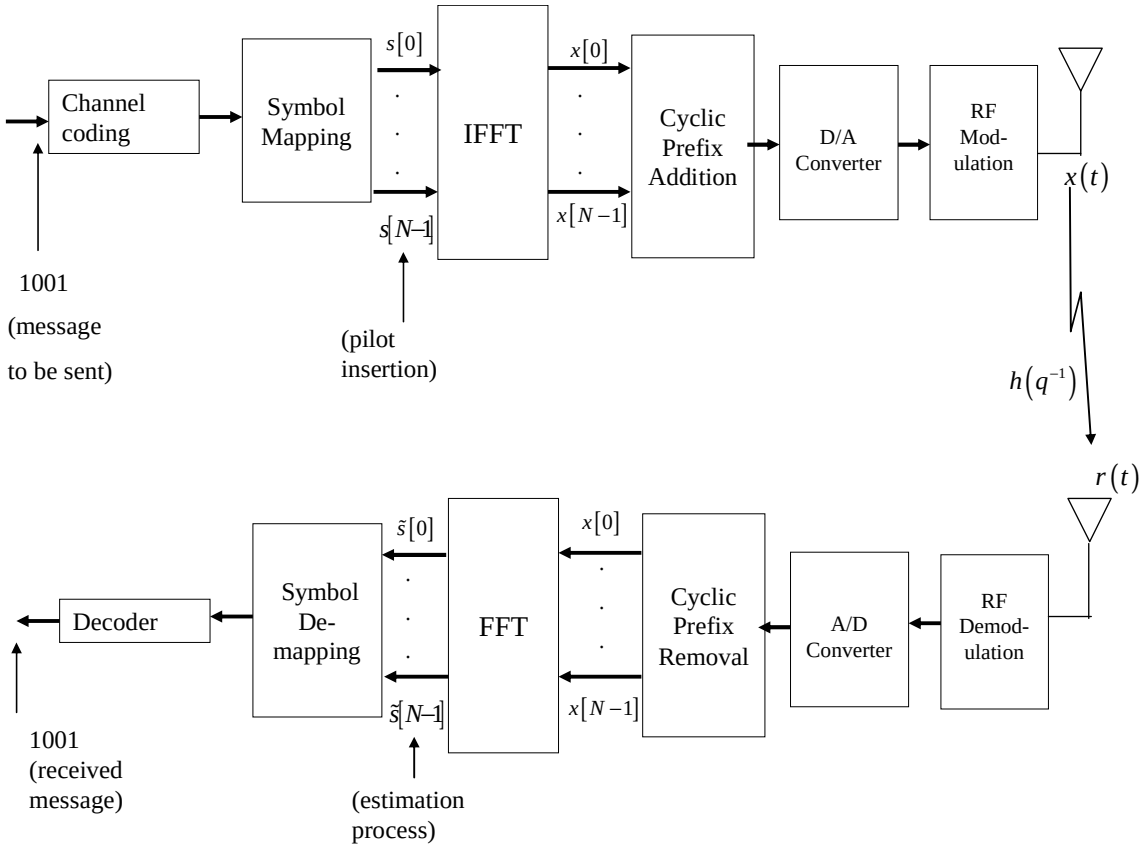

Figure 13. Block Diagram of a SISO-OFDM Scheme

a. Channel Encoding

The information bit sequence is first encoded by the channel encoder. Error control coding is used to rearrange the transmitted information to increase its resistance to noise. The IEEE 802.16a standard uses concatenated forward error correction (FEC), which is based on the serial concatenation of a Reed-Solomon outer code and a rate compatible Trellis coded modulation (TCM) inner code. Between the outer and the inner code, employing an interleaver is optional. Since our main focus in this thesis was to study the MIMO and MIMO-OFDM systems, the simulation only used the convolutional encoder to keep it simple. The encoder had a rate of ½, constraint length 7 and generator polynomials in octal form 171 and 133 [10].

b. Symbol Mapping

The channel encoded bits are mapped to I and Q symbol coordinates using a gray code symbol map depending on the modulation scheme. Figure 14 shows some of the constellations introduced in IEEE 802.16a standard.

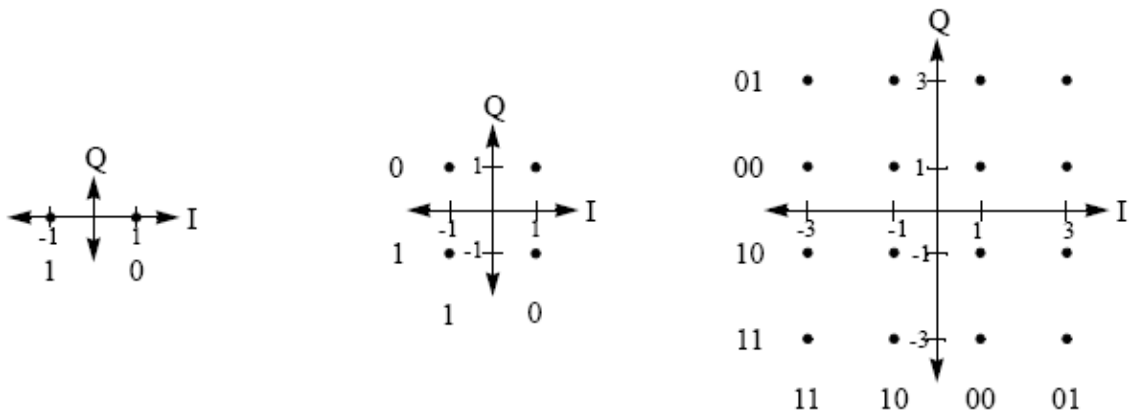

(a) (b) (c)

Figure 14. Gray coded (a) BPSK, (b) QPSK and (c) 16-QAM constellations (From Ref. 10.)

c. Inverse Fast Fourier Transform (IFFT) Operation

Mapped symbols are next input to the IFFT block. The FFT size is equal to the number of subcarriers. In the IEEE 802.16a standard, two types of OFDM schemes are included, OFDM with 256 subcarriers and OFDMA (for higher data rates and multiple access) with 2048 subcarriers. In this thesis, the OFDM with 256 subcarriers was chosen for simulation purposes. Three types of subcarriers are defined in the OFDM technique of IEEE 802.16a standard: data carriers for information transmission, pilot carriers designed to extract the channel information at the receiver, and guard carriers (also called null carriers) placed on the either edge of the spectrum to avoid interference from adjacent bands. The assignment of subcarriers in the IEEE 802.16a standard is given in Table 6. These carrier allocations will be used in organizing the information and pilot symbols before the IFFT operation. Figure 15 illustrates the subcarrier organization prior to IFFT operation according to the carrier allocation given in Table 6.

Size of FFT	256
# of information subcarriers	192
# of pilot subcarriers	8
# of null subcarriers (including the DC subcarrier)	56
# of lower frequency guard subcarriers	28
# of higher frequency guard subcarriers	27
Frequency indices of null subcarriers (including the DC subcarrier)	$-128,-127,\ldots,-101,0$ $+101,+102,\ldots,+127$
Frequency indices of pilot subcarriers	$-84,-60,-36,-12,12,36,60,84$

Table 6. Allocation of OFDM Subcarriers in the IEEE 802.16a Standard

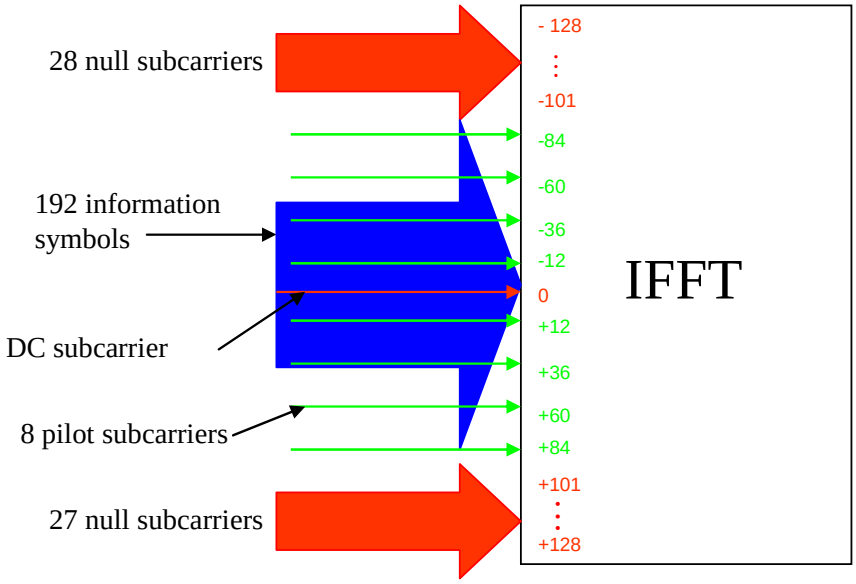

Figure 15. Allocation of Subcarriers before the IFFT Block (see Table 6)

The output of the IFFT block in discrete time can be expressed by

$$x[n]=\frac{1}{\sqrt{N_{FFT}}}\sum_{k=0}^{N_{FFT}-1}s_k e^{j2\pi f_k n} \qquad n=0,1...N_{FFT}-1 \tag{4.16}$$

where s_k is the *k*-th symbol entering to the IFFT block and f_k is the *k*-th subcarrier frequency. The index of subcarrier frequency in (4.16) is chosen to be 0 to $N_{FFT}-1$ instead of -128 to $+128$, for convenience. The length of the IFFT output is called the useful time T_b.

d. Cyclic Prefix Addition

Multipath delay spread causes intersymbol interference (ISI), and the ISI brings about performance degradation. To deal with this problem, a guard time is introduced for each OFDM symbol. The guard time is chosen to be larger than the expected delay spread so that multipath components from one symbol would not interfere with those from the next symbol. In the IEEE 802.16a standard, optional guard lengths T_g are specified with respect to the useful time T_b. The optional guard ratios T_g/T_b are $1/4, 1/8, 1/16$ and $1/32$. The desired length of the guard interval is derived from this ratio. The addition of cyclic prefix (CP) is shown in Figure 16. Consider that the guard ratio is chosen to be $1/16$. The output of the IFFT block has a length of 256; therefore, the guard length will be 16. The CP is formed by taking the last 16 samples of the IFFT output and concatenating them to the beginning of the symbol sequence in (4.16). The resulting new sequence is

$$x_{CP} = \left[x[240] \quad x[241] \quad \ldots \quad x[254] \quad x[255] \quad x[0] \quad x[1] \quad \ldots \quad x[255] \right]. \quad (4.17)$$

The total interval after adding the CP is referred to as the symbol time T_s.

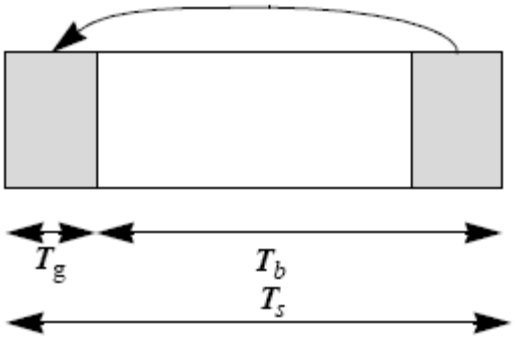

Figure 16. OFDM Symbol Time Structure (From Ref. 10.)

e. Digital-to-Analog Conversion and RF Modulation

After CP addition, the discrete time domain samples are converted to analog signals using a digital-to-analog (D/A) converter. The converted signal is a continuous time baseband OFDM symbol. Then the OFDM symbols are upconverted to a radio frequency carrier, amplified and transmitted through the antenna. The IEEE 802.16a standard is specified for the 2-11 GHz band. In this thesis, the simulations were conducted at the baseband level, i.e., no RF modulation was implemented.

f. RF Demodulation and Digital to Analog Conversion

The transmitted OFDM symbols experience the channel and reach the receiver. Assuming that the channel is modeled as a multitap filter, the transmitted signal is passed through a discrete time filter. The coefficients of the filter are the complex tap values of the channel. The received signal now can be expressed by

$$r(t) = h\left(q^{-1}\right)x(t) \tag{4.18}$$

where $h\left(q^{-1}\right)$ is the discrete-time filter representation of the channel and $x(t)$ is the baseband OFDM symbol transmitted from the antenna.

g. Cyclic Prefix Removal and FFT Operation

The cyclic prefix added at the transmitter is removed to process the needed information. After removal of the CP, we have the 256 samples carrying the transmitted symbol and channel information. These 256 samples are processed through the FFT block, and the information symbols and the channel information are obtained. The estimate of the symbol sent on the *k*-th subcarrier is given by

$$\tilde{s}(k) = H^{*}(k)\hat{r}(k) \tag{4.19}$$

where $H(k)$ is the frequency response of the channel at the *k*-th subcarrier frequency and $\hat{r}(k)$ is *k*-th element of the sequence obtained by the FFT operation. In all simulations, we assumed that there was full channel knowledge at the receiver, i.e., the channel estimation was not performed. The frequency response of the channel $H(k)$ was obtained by taking the discrete Fourier transform of the channel impulse response with an FFT of size 256.

In practice, channel state information is carried to the receiver in the pilot carriers. Since the channel estimation was not included in our simulations, the pilot symbols were set to zero. Hence pilot insertion was not carried out in the simulation steps but left open for future work.

h. Demapping and Decoding

The estimates of the transmitted symbols are then demapped to bits with reference to the constellation and sent to the Viterbi decoder. The Viterbi decoder is used to decode bit streams encoded by the convolutional encoder. A Viterbi decoder searches the trellis to determine the path that can create the bit stream closest to the received one. The measure of closeness can be measured using hard or soft decision decoding techniques. The hard decision decoding technique tries to find the bit stream path that has the minimum Hamming distance from the received sequence. In soft decision decoding, the bit stream path that has the minimum Euclidian distance from the received sequence is computed [17]. In the simulation process, hard decision decoding was employed at the Viterbi decoder. The details of the Viterbi decoder can be found in [18].

2. SIMO-OFDM Systems over Frequency-Selective Channels

Since we have given a detailed explanation for SISO-OFDM systems in the preceding discussion, we will skip the following steps in discussing the MIMO-OFDM systems: channel encoding, symbol mapping, pilot insertion, digital-to-analog conversion, and RF modulation at the transmitter; RF demodulation, analog-to-digital conversion, cyclic prefix, extracting the information symbols from the FFT block, and Viterbi decoding at the receiver. The resulting schematic of a system utilizing OFDM with single transmit antenna and two receive antennas is illustrated in Figure 17.

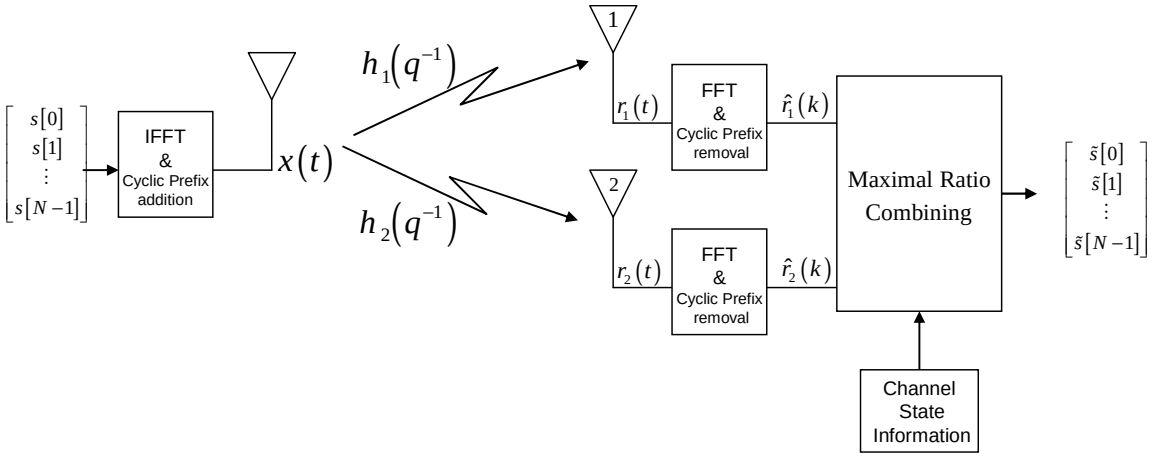

Figure 17. Schematic of a 1×2 SIMO-OFDM System Utilizing MRC

The transmitted OFDM symbol will experience two different channels h_1 and h_2. The received signals are given by

$$\begin{aligned} r_1(t) &= h_1\left(q^{-1}\right)x(t) \\ r_2(t) &= h_2\left(q^{-1}\right)x(t) \end{aligned} \tag{4.20}$$

where $h_1\left(q^{-1}\right)$ and $h_2\left(q^{-1}\right)$ are the discrete-time filter representations of the two SIMO channels and $x(t)$ is the transmitted OFDM signal. At the receiver, the CP is removed and the FFT of the 256 time-domain samples is taken. By using the MRC scheme, the estimate of the transmitted symbol at the *k*-th subcarrier is computed by

$$\tilde{s}(k) = H_1^*(k)\hat{r}_1(k) + H_2^*(k)\hat{r}_2(k) \tag{4.21}$$

where $H_1^*(k)$ and $H_2^*(k)$ are the complex conjugate versions of the frequency responses of the channels at the *k*-th subcarrier, and $\hat{r}_1(k)$ and $\hat{r}_2(k)$ are the *k*-th output of the FFT blocks.

3. MISO-OFDM Systems over Frequency-Selective Channels

A schematic of a MISO-OFDM system with two transmit antennas and a single receiving antenna utilizing STBC is shown in Figure 18. In SISO-OFDM and SIMO-OFDM systems, only one OFDM symbol (carrying 192 information symbols as specified in the IEEE 802.16a standard) is transmitted through a given transmit antenna at a time. Since there are two transmit antennas for the MISO-OFDM, two different OFDM sym-

bols (making it a total of 384 information symbols) are transmitted from the two transmit antennas simultaneously. The STBC encoder performs encoding over two consecutive symbol blocks. The four encoded symbol blocks for transmission are constructed as follows:

$$\begin{aligned} s_1 &= \begin{bmatrix} s[1] & s[2] & \dots & s[192] \end{bmatrix} \\ s_2 &= \begin{bmatrix} s[193] & s[194] & \dots & s[384] \end{bmatrix} \\ s_3 &= \begin{bmatrix} -s^*[193] & -s^*[194] & \dots & -s^*[384] \end{bmatrix} \\ s_4 &= \begin{bmatrix} s^*[1] & s^*[2] & \dots & s^*[192] \end{bmatrix}. \end{aligned} \tag{4.22}$$

This block construction is analogous to the STBC-SC scheme in Section A; therefore, in the literature this scheme is also called STBC-OFDM. The allocation of subcarriers is carried out as specified in the IEEE 802.16a standard for OFDM (see Figure 15).

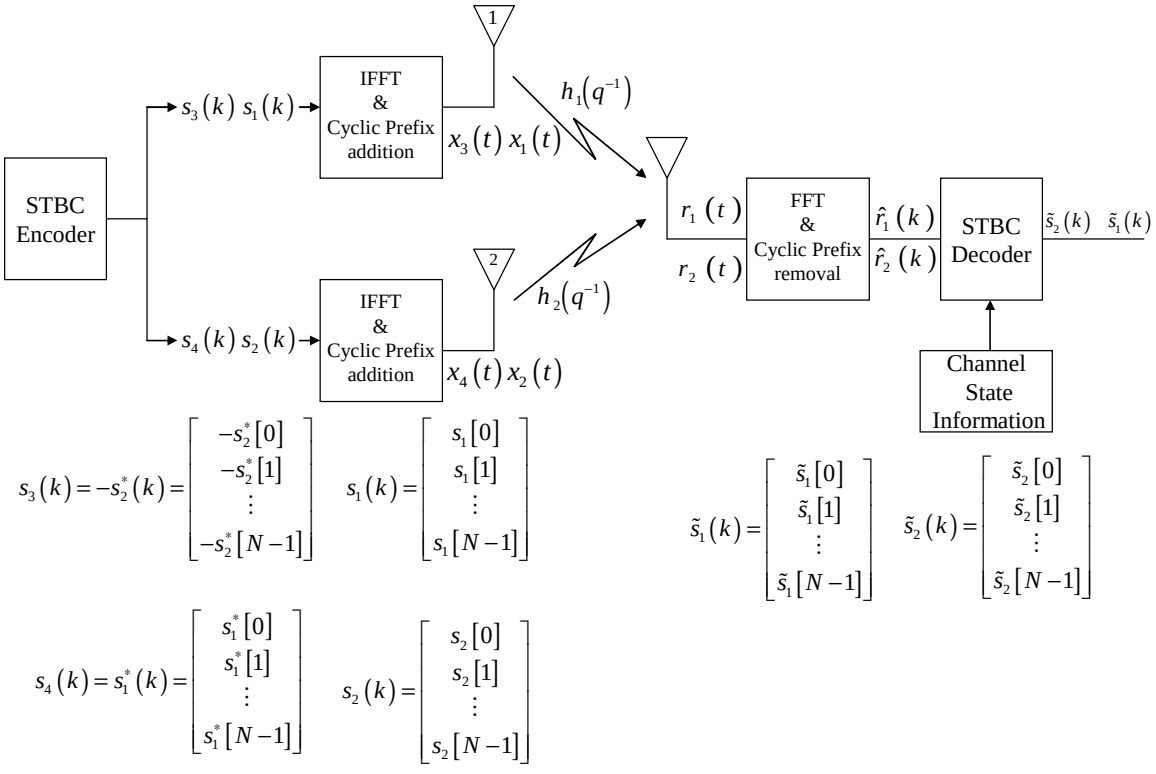

Figure 18. Schematic of a 2×1 MISO-OFDM System Utilizing STBC

Each of the OFDM symbols $x_i(t), i = 1,2,3,4$, contains a block of 192-symbol, $s_i, i = 1,2,3,4$, presented in (4.22), respectively. Assuming that the channel characteris-

tics remain constant over two consecutive OFDM symbols, the received signals are expressed by

$$\begin{aligned} r_1(t) &= h_1\left(q^{-1}\right)x_1(t) + h_2\left(q^{-1}\right)x_2(t) \\ r_2(t) &= h_1\left(q^{-1}\right)x_3(t) + h_2\left(q^{-1}\right)x_4(t) \end{aligned} \tag{4.23}$$

where $h_1\left(q^{-1}\right)$ and $h_2\left(q^{-1}\right)$ are the discrete-time filter representations of the two MISO channels. The STBC decoder at the receiver computes the estimates of the transmitted signal at the *k*-th subcarrier frequency using the decoding equations given by [4, 7]

$$\begin{aligned} \tilde{s}_1(k) &= H_1^*(k)\hat{r}_1(k) + H_2(k)\hat{r}_2^*(k) \\ \tilde{s}_2(k) &= H_2^*(k)\hat{r}_1(k) - H_1(k)\hat{r}_2^*(k) \end{aligned} \tag{4.24}$$

where $H_1^*(k)$ and $H_2^*(k)$ are the complex conjugates of the frequency responses of the channels at the *k*-th subcarrier frequency, and $\hat{r}_1(k)$ and $\hat{r}_2(k)$ are the *k*-th output of the FFT blocks.

4. MIMO-OFDM Systems over Frequency-Selective Channels

A schematic of a MIMO-OFDM system utilizing STBC with two transmit and two receive antennas is shown in Figure 19. The transmitter side of the system is identical to the MISO-OFDM employing STBC. Assuming that the channel characteristics remain constant over the period of two transmission bursts, the received signals are given by

$$\begin{aligned} r_1(t) &= h_{1,1}\left(q^{-1}\right)x_1(t) + h_{2,1}\left(q^{-1}\right)x_2(t) \\ r_2(t) &= h_{2,1}\left(q^{-1}\right)x_1(t) + h_{2,2}\left(q^{-1}\right)x_2(t) \\ r_3(t) &= h_{1,1}\left(q^{-1}\right)x_3(t) + h_{2,1}\left(q^{-1}\right)x_4(t) \\ r_4(t) &= h_{2,1}\left(q^{-1}\right)x_3(t) + h_{2,2}\left(q^{-1}\right)x_4(t) \end{aligned} \tag{4.25}$$

where $h_{i,j}\left(q^{-1}\right),\ i=1,2\ j=1,2$, are the discrete-time filter representations of the channel from the *j*-th transmit antenna to the *i*-th the receive antenna. The STBC decoder at the receiver antenna will estimate the transmitted symbols at the *k*-th subcarrier frequency using the decoding equations given by [4, 7]

$$\begin{aligned} \tilde{s}_1(k) &= H_{1,1}^*(k)\hat{r}_1(k) + H_{1,2}(k)\hat{r}_3^*(k) + H_{2,1}^*(k)\hat{r}_2(k) + H_{2,2}(k)\hat{r}_4^*(k) \\ \tilde{s}_2(k) &= H_{1,2}^*(k)\hat{r}_1(k) - H_{1,1}(k)\hat{r}_3^*(k) + H_{2,2}^*(k)\hat{r}_2(k) - H_{2,1}(k)\hat{r}_4^*(k) \end{aligned} \tag{4.26}$$

where $H_{i,j}(k),\ i=1,2\ j=1,2$, are the frequency response values of the channel from the *j*-th transmit antenna to the *i*-th the receive antenna for the *k*-th subcarrier, and $\hat{r}_i(k),\ i=1,2,3,4$, are the output of FFT blocks at the *k*-th subcarrier.

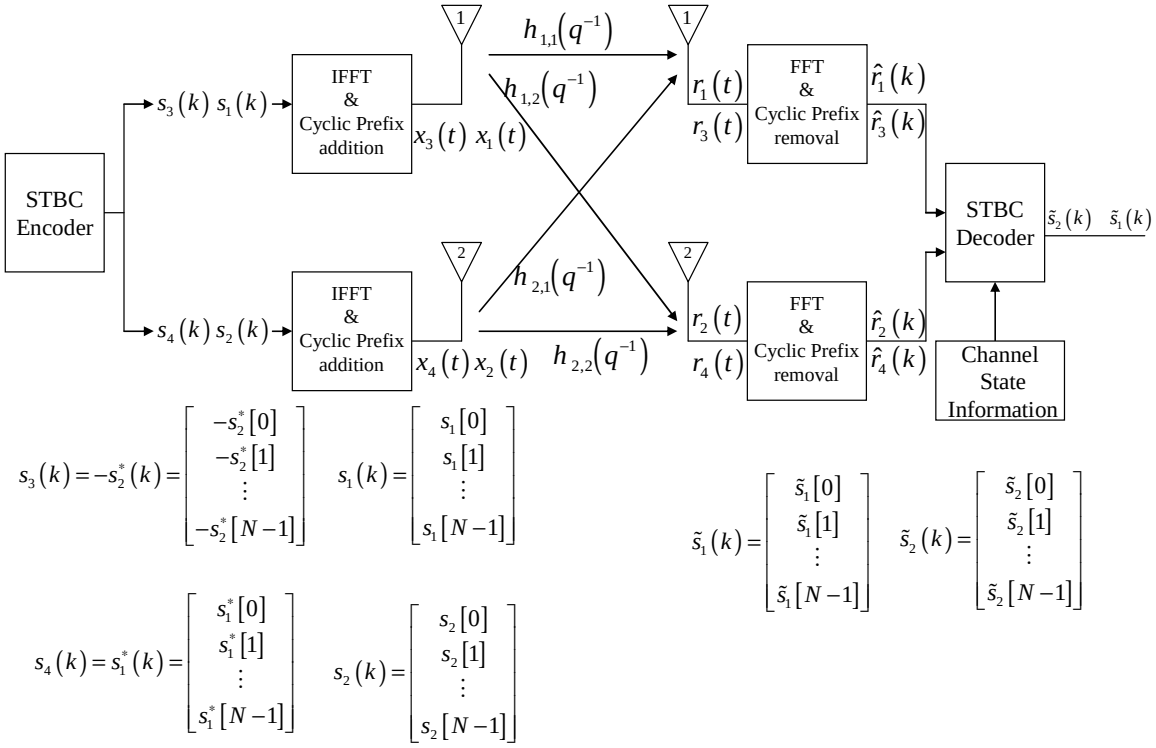

Figure 19. Schematic of a 2×2 MIMO-OFDM System Utilizing STBC

C. SUMMARY

This chapter discussed the MIMO schemes using single-carrier and OFDM modulation over frequency-selective channels. In the presence of a frequency selective channel, STBC was used to realize these MIMO schemes.

The discussion of the single-carrier and OFDM systems was based on the simulation developed in Matlab. While developing the input-output relations and the decoding equations of the systems, the transmitted signals were assumed to be in baseband, i.e., RF modulation was not conducted in the simulations. The channel information given in the decoding equations were based on the assumption that there was full knowledge of the channel characteristics at the receiver, i.e., channel estimation was not performed in the simulation process.

The next chapter discusses the simulation model developed to study MIMO-SC and MIMO- OFDM schemes over the frequency selective SUI channels and presents the simulation results.

V. SIMULATION RESULTS

The previous chapters covered the principles of the Alamouti scheme over flat channels, STBC systems with single-carrier and OFDM modulation. This chapter presents performance comparisons of the MIMO systems developed in Matlab. In the simulation process, the goal was to reach a bit error rate (BER) of at least 10^{-5} to evaluate the performances of the systems. Therefore for each E_b/N_o, at least 1,000,000 information bits were simulated for each system. One run of sending about 1,000,000 bits for all E_b/N_o values is called a Monte Carlo run. The systems were simulated for a specified number of Monte Carlo runs and the results were averaged such that the BER curves were smooth enough for evaluation.

A. PERFORMANCE OF SYSTEMS USING ALAMOUTI SCHEMES

Initially a Matlab code was generated including the SISO (1×1), the SIMO (1×2), the MISO (2×1) and the MIMO (2×2) systems with single-carrier modulation. The Alamouti coding scheme discussed in Chapter II was performed over consecutive symbol pairs. The developed systems were simulated over Rayleigh fading, one tap, zero mean, circularly symmetric and complex valued channels $\mathbf{H}_w$ (see properties of $\mathbf{H}_w$ in (3.1)). For the MISO and the MIMO cases, it was assumed that the channel characteristics remained constant over consecutively transmitted symbol periods. Each channel was generated independently, i.e., it was assumed that the channels in all multiple antenna cases were uncorrelated. For this simulation, channel encoding was not employed. It was assumed that the total transmitted power from two antennas for the MISO and the MIMO systems was the same as the transmitted power from the single antennas for the SISO and SIMO systems. Additionally, we assumed that there was full knowledge of the channel at the receiver. After computing the received signal(s) at the receiver(s), estimates of the transmitted symbols were computed using the relations given in (2.13), (2.17) and (2.20). Table 7 lists the parameters of the simulation run using the QPSK modulation. By using the QPSK modulation, 1,000,000 information bits were mapped into 500,000 symbols. The BER curves were smooth enough for evaluation with 10 Monte Carlo runs.

# of transmitted information bits for each E_b/N_o	1,000,000
# of symbols transmitted for each E_b/N_o	500,000
# of Monte Carlo runs	10

Table 7. Parameters for Alamouti and MRC Single-Carrier Simulations

Figure 20 shows the BER performance of SISO (1×1), SIMO (1×2, MRC), MISO (2×1, Alamouti Scheme) and MIMO (2×2, Alamouti Scheme) systems over Rayleigh fading channels. The performance of the MISO (2×1) is 3 dB worse than the SIMO (1×2), i.e., the performance gap between the two schemes is 3 dB at each E_b/N_o value. This 3 dB gap has occurred because the transmitted power for the MISO system is kept at half the power for the SIMO system. If each antenna of the MISO system had transmitted at the same power level as the single transmit antenna of the SIMO system, the BER curves of these two schemes would be identical. As a result, we have shown that a SIMO system utilizing the MRC scheme is identical to a MISO system employing the Alamouti scheme [4].

On the other hand, both systems have a significant improvement over the SISO system. Increasing the number of antennas either at the transmitter or the receiver gave spatial diversity gain. Even at a BER of 2×10^{-3}, the MISO system performs approximately 10 dB better than the SISO system. By observing the slope of the curves, we can remark that for higher E_b/N_o, the gap will increase. Adding one more transmit antenna to the SIMO system gave us more gain. Although the transmitted power was halved, the MIMO system has about 10 dB better performance than the SIMO system at a BER of 10^{-5}. As E_b/N_o is increased, the performance gap increased as well.

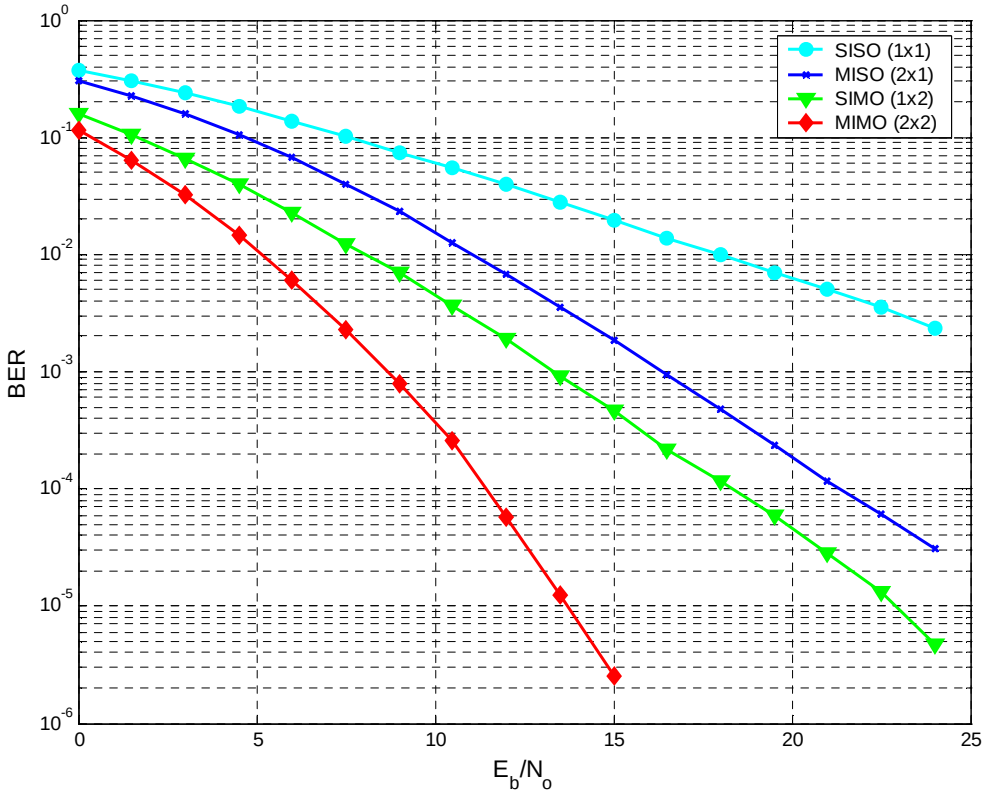

Figure 20. The BER Performance Comparison of the Alamouti Schemes to the MRC Scheme over Rayleigh Fading Channels (The simulation parameters are given in Table 7)

B. PERFORMANCE OF MIMO-SC SYSTEMS OVER SUI CHANNELS

We discussed the SUI channels in Chapter III and the STBC-SC schemes in Chapter IV. The parameters in STBC-SC simulations were chosen to be comparable to the OFDM parameters of the IEEE 802.16a standard since we wanted to compare the performances of the single-carrier schemes to the OFDM schemes. To simulate the STBC schemes, a Matlab code was generated. The generation of the SUI channels was achieved with the modified version of the Matlab code presented in [11]. The output of the channel generation code was three complex numbers that represent the three-tap SUI channels. A sampling operation was carried out to implement the generated SUI channels. The sampling frequency $f_s = 22.857$ MHz was chosen based on the IEEE 802.16a standard specification. The derivation of f_s will be discussed later in the OFDM simulation sec-

tion. In STBC, space coding was performed over two consecutive blocks of symbols as discussed in Chapter III. To make a fair comparison of the single-carrier schemes to the OFDM systems, the block size was chosen as 192 since the number of information symbols transmitted in an OFDM symbol is 192.

After setting the sampling frequency and the symbol block size, discrete-time domain representations of the SUI channels were investigated. Figure 21 shows the three-tap SUI channels with sampling frequency $f_s = 22.857$ MHz. This figure highlights the different delay spreads encountered by different SUI channels. For example, the SUI-3 channel model has a second tap at $t = 0.4\,\mu$s and a third tap $t = 0.9\,\mu$s. All other samples were set to zero in the sequence of the sampled channel. In the implementation, the delay spread parameters matched the SUI channel parameters shown in Appendix A. Notice that SUI-5 and SUI-6 have delay spreads up to 10 μs and 20 μs, respectively.

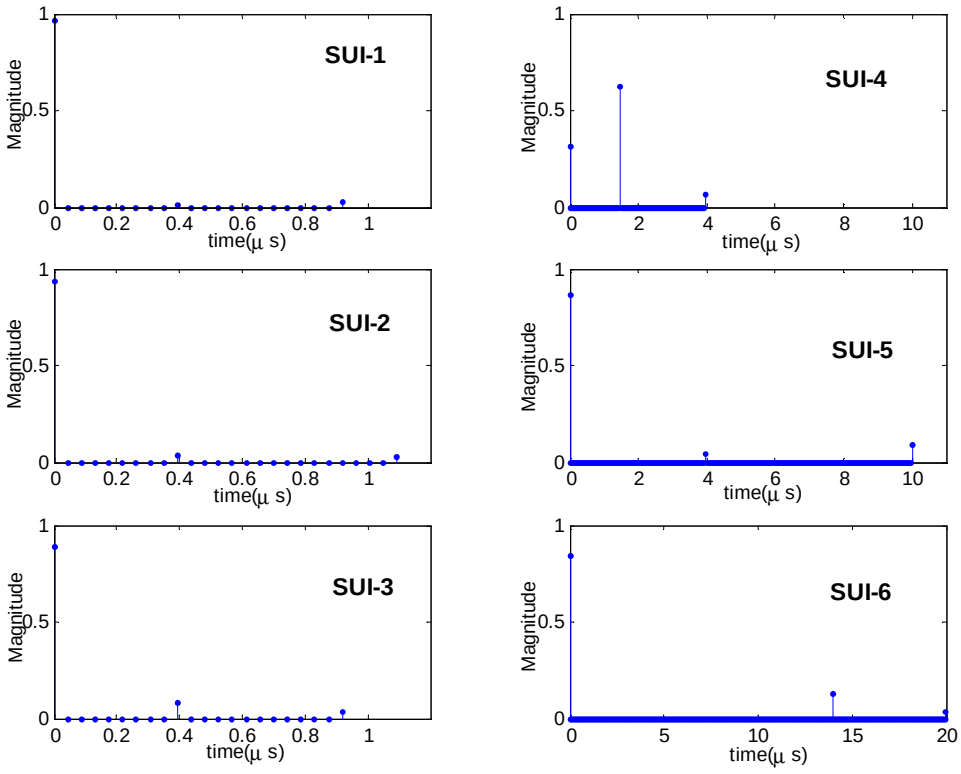

Figure 21. SUI Channel Impulse Responses on a Sampling Grid with a Sampling Frequency $f_s = 22.857$ MHz

The next step was to simulate the SISO system over different SUI channels. The generation of the 192-symbol block is illustrated in Figure 22. The implementation utilizes a rate ½ convolutional encoder. Consequently, 192 information bits were mapped into 192 QPSK symbols. The simulation parameters for the system using the QPSK modulation are listed in Table 8. In line with the generation process shown in Figure 22, 1,536,000 information bits were mapped into 4000 symbol blocks of length 192. In the simulation, it was assumed that the channel characteristics remained constant over the transmission period of a 192-symbol block.

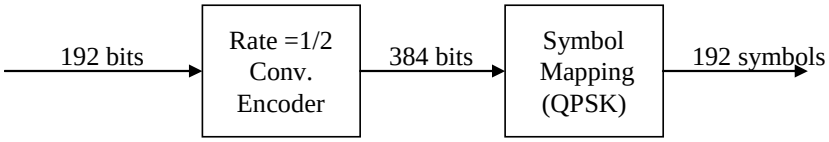

Figure 22. Schematic of Generation of 192-symbol Blocks

# of transmitted information bits for each E_b/N_o	1,536,000
# of symbol blocks transmitted for each E_b/N_o	4000
Convolutional Encoder generator polynomials	171,133
# of Monte Carlo runs	30

Table 8. Parameters for SISO System Simulations over SUI Channels

The received signals and the estimates of the transmitted symbols were computed using the relations given in (4.3) and (4.4), respectively. The BER performance plots of the SISO system utilizing QPSK over AWGN and SUI-1 to SUI-6 channels are shown in Figure 23. Not surprisingly the system has the best performance in AWGN. As the system experiences higher SUI channels, the BER performance gets worse. The SUI-3, 4, 5 and 6 channels cause considerable performance degradation. On the other hand, the SUI-1 and the SUI-2 channels have less severe effects on the system. In the remaining simulations, SUI-2 channel is used to study the performance of the MIMO systems. SUI-4, 5 and 6 are not further considered here because of their larger delay spreads ($4-20\ \mu$s). SUI-2 is a reasonable channel model for an overall performance study since it accounts for multipath and yet has a stronger direct signal compared to SUI-3.

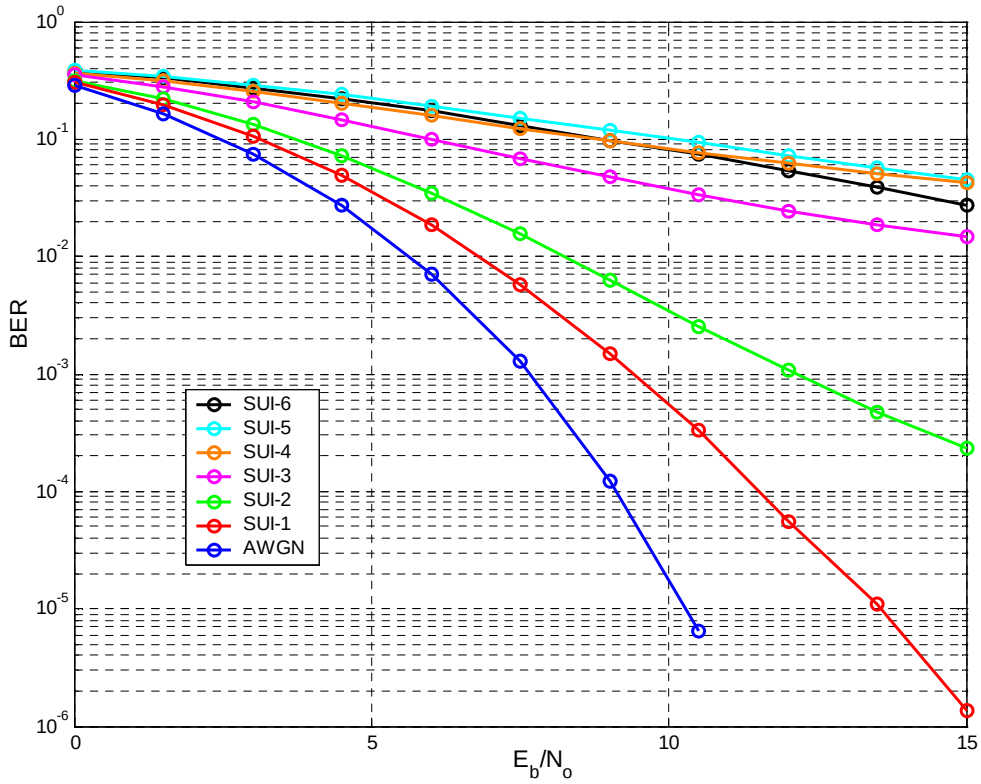

Figure 23. The BER Performance of the SISO-SC System over Different SUI Channels (The simulation parameters are given in Table 8)

After selecting the SUI-2 channel as the simulation environment, all STBC systems with single-carrier were simulated over the SUI-2 channel. For the MISO and the MIMO systems, the 192-symbol blocks were generated as illustrated in Figure 24. By using a rate ½ convolutional encoder, 384 information bits are mapped into 384 QPSK symbols, which are then divided into two symbol blocks, one for each antenna. The simulation parameters of the single-carrier schemes are listed in Table 9. As investigating the performance of STBC-SC schemes was one of the major goals of this work, the number of information bits and the number of Monte Carlo runs were chosen to be higher than those of the previous simulations. By choosing a higher number of bits, we aimed to measure the bit error performance at lower rates.

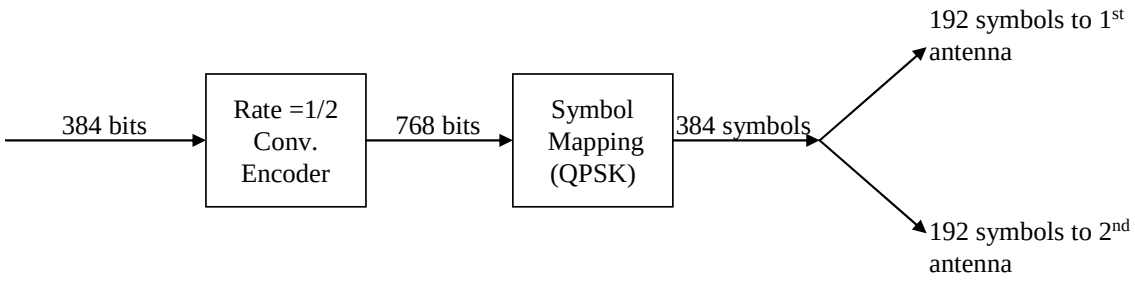

Figure 24. Schematic of Generation of 192-symbol Blocks for each Transmit Antenna

# of transmitted information bits for each E_b/N_o	3,840,000
# of symbol blocks transmitted for each E_b/N_o	10,000
Convolutional Encoder generator polynomials	171,133
# of Monte Carlo runs	50

Table 9. Parameters for Simulations of the Single-Carrier Systems over SUI-2 Channel

In the simulations, it was assumed that we had the perfect channel knowledge at the receiver. We also assumed that the channel characteristics remained constant over two transmission burst periods for the MISO and MIMO systems. The total transmitted power is kept at the same level for all schemes, i.e., for the MISO and the MIMO cases the power for each antenna is halved as compared to the SIMO and SISO cases.

The equations used to compute the received signals and estimates in the simulation are (4.3)-(4.4), (4.6)-(4.7), (4.11)-(4.12) and (4.25)-(4.26) for SISO-SC (1×1), SIMO-SC (1×2), MISO-SC (2×1) and MIMO-SC (2×2) systems, respectively.

The simulation results of all single-carrier schemes are shown in Figure 25. The 3 dB performance gap between the MISO and the SIMO systems was observed again. The MIMO-SC outperformed all other schemes. At a BER of 10^{-4}, MIMO-SC performed better than the SIMO-SC by about 1.0 dB. The performance gap is increased as E_b/N_o is increased. The performance gap is about 2.5 dB at a BER of 2×10^{-6}. The largest gap is certainly between the SISO-SC and the MIMO-SC. At a BER of 6×10^{-5}, the MIMO-SC

outperforms the SISO-SC by approximately 11 dB. This result showed that adding more antennas at both ends of the communication link gave us significant performance improvement.

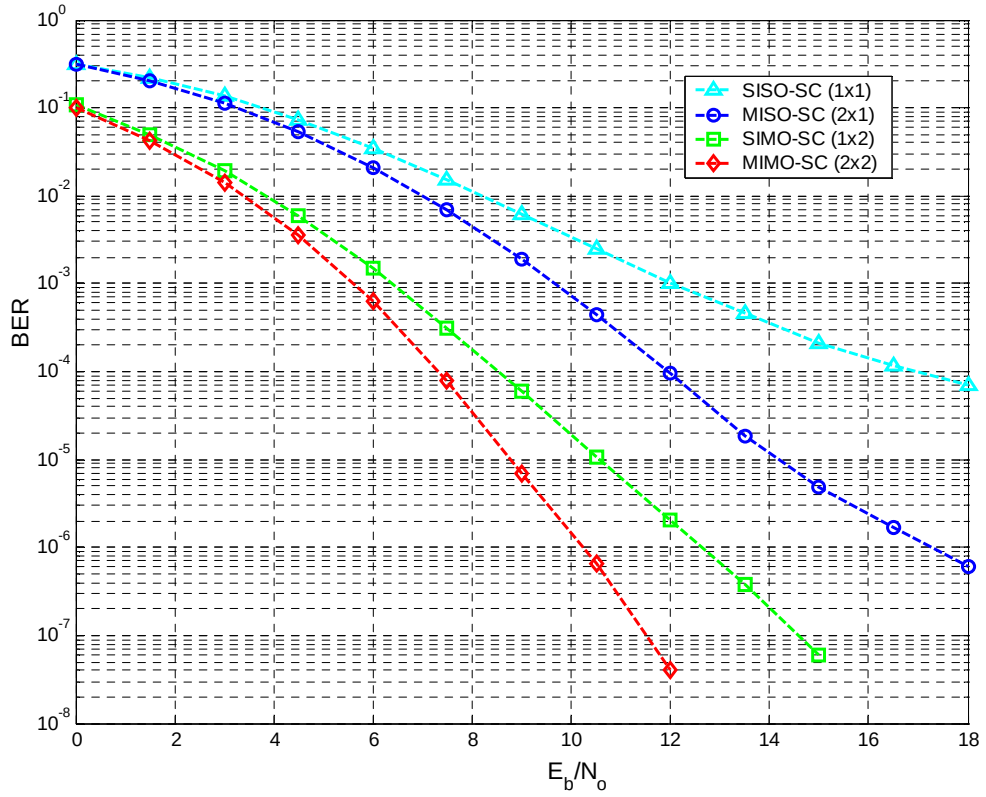

Figure 25. The BER Performance Comparisons of Single-Carrier Schemes over the SUI-2 Channel (The simulation parameters are given in Table 9)

The next simulation was conducted to observe the effects of spatial correlation on the single-carrier systems. The SISO and the MISO systems were chosen for examining the correlation effects. The BER performance of the MISO system with different transmit correlation coefficients ρ_t is compared to that of the SISO case. The transmit correlation matrix was constructed as given in (3.5). The correlated MISO channel was rebuilt with the relation given in (3.8). The simulation parameters of the MISO system over the correlated channel are listed in Table 10. By using the QPSK modulation, 1,536,000 information bits were mapped into 8000 symbols blocks, each of length 192. The BER curves were plotted based on 30 Monte Carlo runs.

# of transmitted information bits for each E_b/N_o	1,536,000
# of symbol blocks transmitted for each E_b/N_o	8,000
Convolutional Encoder generator polynomials	171,133
# of Monte Carlo runs	30

Table 10. Parameters for Simulations of the MISO System over Correlated SUI-2 Channels

The BER performance of the MISO single-carrier system over correlated channels is shown in Figure 26. At a BER of 2×10^{-4}, the MISO system performed about 4 dB better than the SISO system over uncorrelated channels. As the correlation coefficient increased, the BER got worse. For example, when $\rho_t = 0.9$ the performance gap at the BER of 2×10^{-4} decreased to 2 dB. As a result, correlation between the channels caused significant performance degradation on the systems with multiple antennas. The correlation coefficients ρ_t and ρ_r mostly depend on the spatial parameters, such as distance between the antennas and the wavelength. Therefore, placing the antennas and selecting the wavelength play important roles on the performance of the systems.

C. PERFORMANCE OF MIMO-OFDM SYSTEMS OVER SUI CHANNELS

The final goal of this thesis was to investigate the performance of MIMO-OFDM systems. The OFDM parameters were chosen from the IEEE 802.16a standard. The parameters in the IEEE 802.16a standard were specified for various bandwidths. For this thesis, the bandwidth (*W*) was chosen as 20 MHz for a license-exempt band. The sampling frequency f_s was derived from the ratio [10]

$$\frac{f_s}{W} = \frac{8}{7}. \tag{5.1}$$

Substituting $W = 20$ MHz into (5.1), the sampling frequency was determined to be

$$f_s = 22.857 \text{ MHz}. \tag{5.2}$$

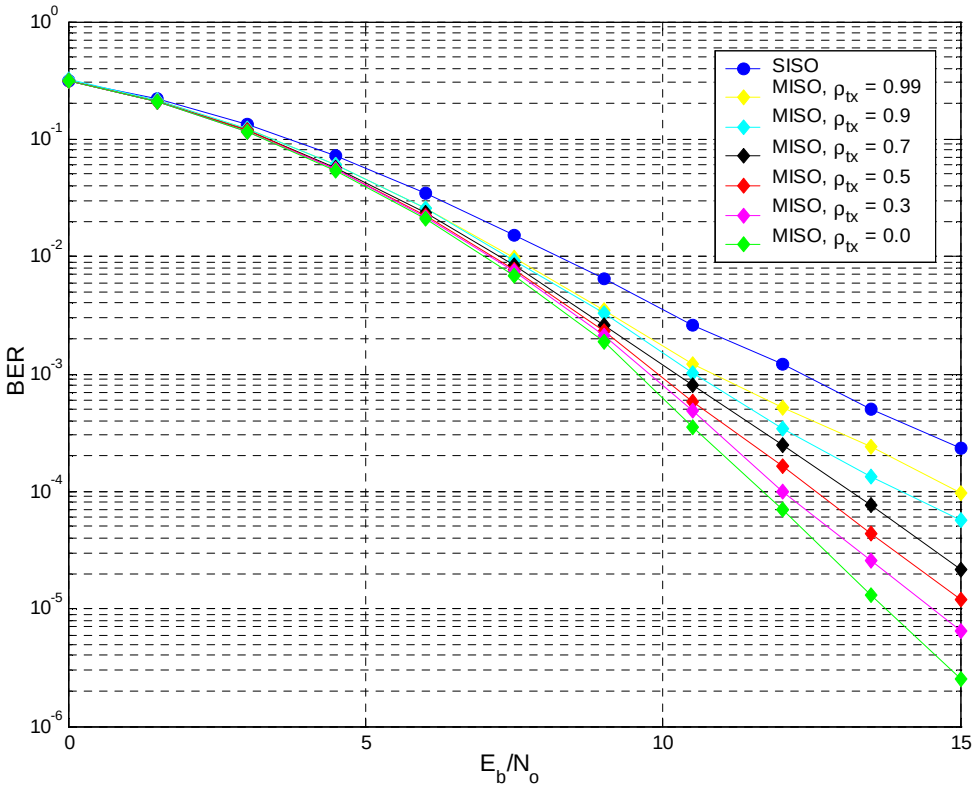

Figure 26. The BER Performance of the MISO Single-Carrier System over Correlated Channels (The simulation parameters are given in Table 10)

The sampling frequency is the most important parameter in the simulation, because the sampling of the impulse response of the three-tap SUI channel, subcarrier spacing, useful time, guard interval and the symbol duration are all based upon it. The carrier spacing was derived from the relation

$$\Delta f = \frac{f_s}{N_{FFT}} \tag{5.3}$$

where N_{FFT} is the FFT size. Substituting $N_{FFT} = 256$ and $f_s = 22.857$ MHz, the carrier spacing was calculated to be

$$\Delta f = 89.3 \text{ kHz}. \tag{5.4}$$

The useful time T_b was computed with the relation

$$T_b = \frac{1}{\Delta f} = 11.2\ \mu s. \tag{5.5}$$

The total OFDM period is given to be

$$T_s = T_g + T_b \tag{5.6}$$

where T_g is the guard interval in an OFDM symbol. The guard interval is determined from the optional guard ratios T_g/T_b. Table 11 lists the OFDM symbol durations for various guard ratios, which range for 1/32 to 1/4. By choosing the smallest guard ratio $T_g/T_b = 1/32$, the total OFDM symbol duration T_s is pretty close to the useful time $T_b = 11.2\ \mu s$. As the guard ratio T_g/T_b increases, the length of CP and OFDM symbol also increases. The guard time (i.e., the CP length) is chosen to be larger than the expected delay spread of the channel so that multipath components from one symbol would not interfere with those from the next symbol. In choosing the guard time, we trade-off between robustness against multipath and bandwidth efficiency. To mitigate the effects of multipath, a large guard time can be chosen, which, on the other hand, it requires wider bandwidth.

Guard Ratio T_g/T_b	**CP length with respect to the FFT size** $N_{FFT} = 256$	**OFDM symbol duration** T_s
1/32	8	11.55 μs
1/16	16	11.9 μs
1/8	32	12.6 μs
1/4	64	14.0 μs

Table 11. OFDM Symbol Durations for Various Guard Ratios

After selecting the OFDM channelization parameters, a SISO-OFDM system was simulated and the performances were compared to those of the SISO-SC system. The SISO-OFDM system was simulated without CP and with the largest guard ratio $T_g/T_b = 1/4$, i.e., from Table 11 the CP size is 64. The simulation parameters are listed in

Table 12. By using the QPSK modulation, 1,536,000 information bits were mapped into 8,000 symbols blocks of length 192 and 8,000 OFDM symbols.

# of transmitted information bits for each E_b/N_o	1,536,000
# of symbol blocks transmitted for each E_b/N_o	8,000
# of OFDM symbols transmitted for each E_b/N_o	8,000
Convolutional Encoder generator polynomials	171,133
# of Monte Carlo runs	30

Table 12. Parameters for Simulations of the SISO-SC and SISO-OFDM Systems over the SUI-2 Channel Model

The BER comparison of SISO-OFDM to the SISO-SC is shown in Figure 27. The SISO-OFDM system without CP has about 1 dB better performance at the BER of 10^{-3} when compared to the SISO-SC. For lower bit error rates, the performance of the SISO-OFDM gets much better. At a BER of 10^{-5}, the performance difference is about 6 dB although no CP was added at the transmitter. This result is due to the SISO-OFDM system's robust performance over frequency selective channels compared to the SISO-SC scheme. When the guard ratio was chosen as $1/4$, the BER curve moved to left about 1 db.

The last step was to present all multiple antenna schemes in one graph. To make a fair comparison, the symbol block size of the single-carrier scheme was selected to be 192. The guard ratio T_g/T_b in all the OFDM schemes was chosen to be $1/4$. For all multiple transmit antenna schemes (MISO-SC, MISO-OFDM, MIMO-SC, MIMO-OFDM), the transmitted power from each antenna is halved when compared to the single transmit antenna schemes (SISO-SC, SISO-OFDM, SIMO-SC, SIMO-OFDM). The channel characteristics were assumed to be constant over consecutive bursts of symbol blocks or OFDM symbols. The multiple channels were generated independently, i.e., it was assumed that all channels were uncorrelated.

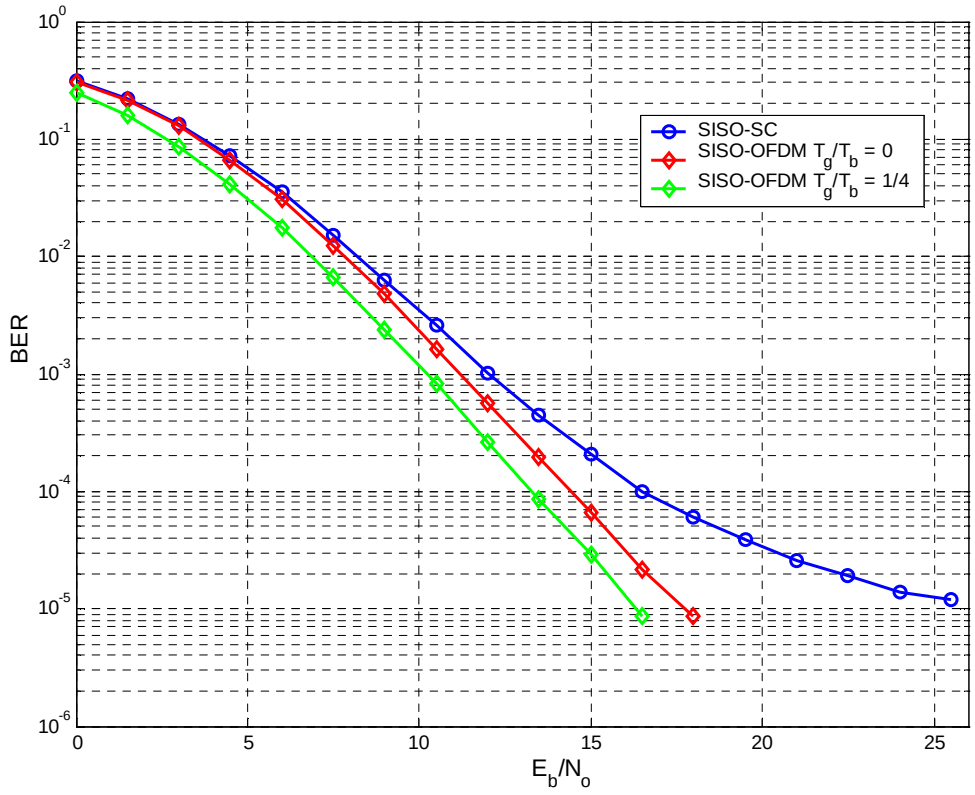

Figure 27. The BER Comparison of SISO-OFDM with Various CP Sizes to SISO-SC over the SUI-2 Channel (The simulation parameters are given in Table 12)

The equations used to compute the received signals and estimates in the simulation are (4.18)-(4.19), (4.20)-(4.21), (4.23)-(4.24) and (4.25)-(4.26) for SISO-OFDM (1×1), SIMO-OFDM (1×2), MISO-OFDM (2×1) and MIMO-OFDM (2×2) systems, respectively.

The simulation parameters for all schemes are listed in Table 13. The parameters were chosen to be of the same as in the single-carrier simulation (see Table 9). By choosing the QPSK simulation, 3,840,000 information bits were mapped into 10,000 OFDM symbols and 192-symbol blocks.

The BER plots for all schemes are shown in Figure 28. The dashed lines are for the SC schemes and the solid lines are for the OFDM schemes. Obviously the MIMO-OFDM system outperforms all other schemes by reaching a BER of 10^{-5} with

$E_b/N_o = 7.5$ dB . When the MIMO-OFDM is compared to the worst performing system, SISO-SC, the performance difference is about 12 dB at a BER of 10^{-4}. The 3-dB gap is again observed between the SIMO-OFDM and the MISO-OFDM systems. Although there are totally three antennas used in the SIMO-OFDM system, the SIMO-OFDM performs better than MIMO-SC (totally four antennas) until the BER is about 10^{-5}. The performance of the two schemes is fairly close after this BER crossover point.

# of transmitted information bits for each E_b/N_o	3,840,000
# of symbol blocks transmitted for each E_b/N_o	10,000
# of OFDM symbols transmitted for each E_b/N_o	10,000
Convolutional Encoder generator polynomials	171,133
# of Monte Carlo runs	50

Table 13. Parameters for Simulations of the all Single-Carrier and OFDM Systems over the SUI-2 Channel

D. SUMMARY

This chapter has presented the simulation results of several Matlab-based communication systems. Simulations were performed over three main steps. First, the Alamouti-scheme-based MIMO systems were simulated over Rayleigh fading, single tap, zero mean and circularly symmetric channels. Next, the simulations of all single-carrier systems over frequency-selective SUI channels were conducted. Lastly, all OFDM systems were simulated. As expected, overall the systems with more antennas performed better than the systems with fewer antennas. Another expected result was that the OFDM systems performed better than the systems utilizing single-carrier modulation.

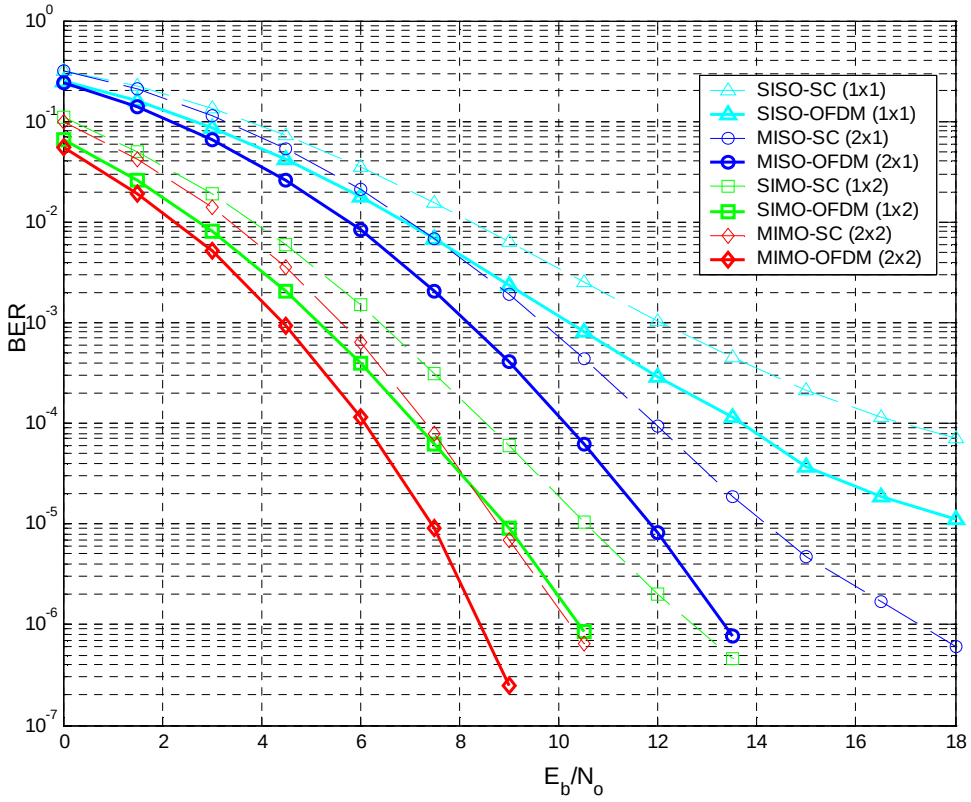

Figure 28. The BER Comparison of all Schemes over the SUI-2 Channel (The simulation parameters are given in Table 13)

THIS PAGE INTENTIONALLY LEFT BLANK

VI. CONCLUSION

The goal of this thesis was to compare the performance of MIMO systems to the conventional SISO systems. This goal was accomplished by investigating the STBC technique and the corresponding decoding algorithms. The investigated space time coding techniques were combined with OFDM to develop the MIMO-OFDM systems and the BER performance of these systems were obtained through a comprehensive simulation study.

A. SUMMARY OF THE WORK DONE

A comprehensive background of the MIMO systems was presented, including the input-output relations, space-coding techniques over flat and frequency selective channels and the decoding algorithms. The presented schemes were investigated for both the single-carrier and the OFDM modulation cases. For the simulation environment, the frequency-selective SUI channels were utilized.

Matlab-based MIMO-SC and MIMO-OFDM communication systems were developed. The simulations were performed for both uncorrelated and correlated MIMO channels based on the SUI models. Simulation results were presented in the form of the BER performance curves and compared among the various MIMO systems studied in this work.

B. SIGNIFICANT RESULTS AND CONCLUSIONS

The most significant result of this study was the observation that the system performance improved as the number of antennas at either side of the communication system was increased. As more antennas were added to the conventional single antenna systems, higher diversity gains improved the performance. Obviously, the system with the largest number of antennas, i.e., the 2×2 system in this work, outperformed all other systems with fewer antennas by exploiting the spatial diversity gain.

The 3-dB penalty for the MISO systems utilizing STBC when compared to the SIMO systems utilizing MRC was observed in all single-carrier and OFDM schemes. This penalty has occurred because the transmitted power for each antenna was halved for the MISO systems when compared to the transmitted power for the SIMO systems. On

the other hand, if the total transmitted power is doubled for the MISO system, then its performance was found to be identical to the SIMO system. In general, building multiple antennas at the base stations (i.e., at the transmitter) is more feasible than building multiple antennas at the mobile stations (i.e., at the receiver) [4]. Moreover, to achieve the same performance, having multiple antennas at the base station is much more profitable than having multiple antennas at all mobile stations.

The other significant result was that the combination of OFDM and MIMO yielded significant performance improvement over frequency-selective multipath channels. Increasing the number of antennas at both/either the receiver and/or the transmitter added more gain to the OFDM systems. The use of multiple antennas added spatial diversity gain to the conventional single-antenna OFDM systems. Therefore, MIMO-OFDM systems appear to be attractive for future wireless communication systems.

C. SUGGESTIONS FOR FUTURE WORK

There are four areas identified for future work. First, the channel information can be extracted from the pilot carriers at the receiver. In all simulations, we assumed that there was perfect channel knowledge at the receiver. Especially for the OFDM simulations, having known the channel (i.e., all three taps of the SUI channels) helped us to compute the exact frequency response of the channel at all 256 subcarrier frequencies. Therefore, in the decoding process for all schemes, perfect channel knowledge boosted the performance. In practice, the channel information must be estimated by using the pilot subcarriers. Accordingly, the frequency response of the channel is known at the receiver with some inaccuracies. These inaccuracies may lead to performance degradation. In this work, while computing the IFFT in the Matlab code, the pilot symbols were set to null. These null spaces may be filled with pilot symbols and the performance of the MIMO systems may be investigated with the channel information extracted from the pilot subcarriers.

A more extensive channel encoder may be used. The specifications for the OFDM systems were chosen from the IEEE 802.16a standard. Although the concatenated FEC encoders or block turbo encoders were introduced in the standard, only a rate ½ convolu-

tional encoder was used in all simulations in this work. Therefore, the Matlab code may be enhanced with a concatenated channel encoder.

In the correlated MIMO channels, the correlation coefficients ρ_t and ρ_r were chosen arbitrarily in this thesis. In the literature, several authors investigated the correlated MIMO channels [14, 19-22]. New Matlab code may be generated to compute the correlation coefficients with respect to the antenna spacing, wavelength, the angle of arrival and the angle of departure of the electromagnetic waves.

Lastly, the number of antennas, either at the receiver or at the transmitter, may be increased. The space coding techniques for higher number of antennas based on the Alamouti scheme were investigated by [23**,** 24]. With higher number of antennas, the decoding equations will be much more complicated but performance improvements may be achieved due to possible spatial diversity gain.

THIS PAGE INTENTIONALLY LEFT BLANK

APPENDIX A. SUI CHANNEL PARAMETERS

This appendix lists the SUI channel parameters. Each channel model has different parameters for the omni and 30° directional antenna systems. The 2^{nd} tap power of the 30° directional channel is attenuated by 6 dB and the 3^{rd} power is attenuated by an additional 12 dB compared to the omnidirectional cases. *K*-factors are defined for 90% and 75% cell coverage. Only the 90% coverage parameters are shown here. More detailed channel parameters are available in [11].

SUI-1 Channel				
	Tap-1	Tap-2	Tap-3	Units
Delay	0	0.4	0.9	μs
Power (omni ant.)	0	-15	-20	dB
Power (30 ant.)	0	-21	-32	dB
K-factor (omni ant.)	4	0	0	dB
K -factor (30 ant.)	16	0	0	dB
Doppler	0.4	0.3	0.5	Hz

SUI-2 Channel				
	Tap-1	Tap-2	Tap-3	Units
Delay	0	0.4	1.1	μs
Power (omni ant.)	0	-12	-15	dB
Power (30 ant.)	0	-18	-27	dB
K -factor (omni ant.)	2	0	0	dB
K -factor (30 ant.)	8	0	0	dB
Doppler	0.2	0.15	0.25	Hz

SUI-3 Channel				
	Tap-1	Tap-2	Tap-3	Units
Delay	0	0.4	0.9	μs
Power (omni ant.)	0	-5	-10	dB
Power (30 ant.)	0	-11	-22	dB
K -factor (omni ant.)	1	0	0	dB
K -factor (30 ant.)	3	0	0	dB
Doppler	0.4	0.3	0.5	Hz

SUI-4 Channel				
	Tap-1	Tap-2	Tap-3	Units
Delay	0	1.5	4	μs
Power (omni ant.)	0	-4	-8	dB
Power (30 ant.)	0	-10	-20	dB
K -factor (omni ant.)	0	0	0	dB
K -factor (30 ant.)	1	0	0	dB
Doppler	0.2	0.15	0.25	Hz

SUI-5 Channel				
	Tap-1	Tap-2	Tap-3	Units
Delay	0	4	10	μs
Power (omni ant.)	0	-5	-10	dB
Power (30 ant.)	0	-11	-22	dB
K -factor (omni ant.)	0	0	0	dB
K -factor (30 ant.)	0	0	0	dB
Doppler	2	1.5	2.5	Hz

SUI-6 Channel				
	Tap-1	Tap-2	Tap-3	Units
Delay	0	14	20	μs
Power (omni ant.)	0	-10	-14	dB
Power (30 ant.)	0	-16	-26	dB
K -factor (omni ant.)	0	0	0	dB
K -factor (30 ant.)	0	0	0	dB
Doppler	0.4	0.3	0.5	Hz

Table 14. Parameters of the SUI Channel Models

APPENDIX B. MATLAB CODE EXPLANATION

This appendix briefly explains the Matlab code, the function of each m-file, and the interrelationships.

To simulate the discussed schemes, two outer functions were generated. The function *alamouti_schemes_over_rayleigh.m* was used for simulating the single-carrier Alamouti schemes over Rayleigh fading channels. For simulating the single-carrier and the OFDM schemes over the SUI channels, the function a*ll_ofdm_and_single_carrier _schemes.m* was used.

A. SIMULATION PARAMETERS

Each function starts by reading the simulation parameters. The simulation parameters are divided into four sections: main parameters, channel parameters, noise parameters, and channel encoder parameters.

The variables in each parameter section are listed in Table 15. The total number of information bits to be transmitted for the given E_b/N_o value can be chosen such that the resulting BER rates are satisfactory for evaluation. In the simulations, it was chosen to be at least 1,000,000 to reach bit error rates on the order of 10^{-5}. For the OFDM and single-carrier simulations over SUI channels, it was chosen to be a multiple of $192\times\log_2(M)$ to match the 192-symbol block size.

The number of Monte Carlo runs were controlled by the variable ‘MonteCarlo’. Before choosing ‘MonteCarlo’, it is recommended that the Profiler function of Matlab be used. By setting up the ‘MonteCarlo’ as 1, the total time of the desired simulation can be measured. Then, the expected time of the simulation can be estimated easily, for larger number of Monte Carlo runs.

Main Parameters	
N	FFT size
M	*m*-ary PSK constellation
N	total number of information bits to be transmitted for the given E_b/N_o value
Tg_rate	CP rate with respect to the FFT size
MonteCarlo	number of Monte Carlo runs to be simulated
EbNo_db	E_b/N_o interval to be simulated (in dB)
Channel Parameters	
SUI_index	SUI model index, from 1 – 6
direct	antenna directivity, omni antenna = 0, 30 deg directional = 1
rho_tx	ρ_t transmit correlation coefficient
rho_rx	ρ_r receive correlation coefficient
fs	sampling frequency
Noise Parameters	
sig	standard deviation of the noise sequence
No	linear noise power
No_db	noise power in dB
Convolutional Encoder Parameters	
constlen	constraint length
codegen	generator polynomials in octal form
trel	trellis description of the encoder

Table 15. The Variables Representing the Simulation Parameters

B. CONDUCTED ITERATIONS

After the system is configured with these parameters, three main iterations start. A conceptual diagram of the iterations and the steps taken in each iteration are shown in Figure 29. The main iteration is the Monte Carlo iteration controlled by the variable 'MonteCarlo'. The next iteration is the E_b/N_o iteration controlled by the variable 'EbNo_db'. The most inner loop is the bit iteration controlled by the variable 'n'. From Figure 29, all system steps are conducted in the bit iteration. In other loops, such as Monte Carlo and E_b/N_o iterations, the number of bit errors are summed up and saved for computing the bit error rate subsequently. The numbers of bit errors are saved until the Monte Carlo loop ends. To compute the BER, the total number of errors is simply divided by the iterated number of bits.

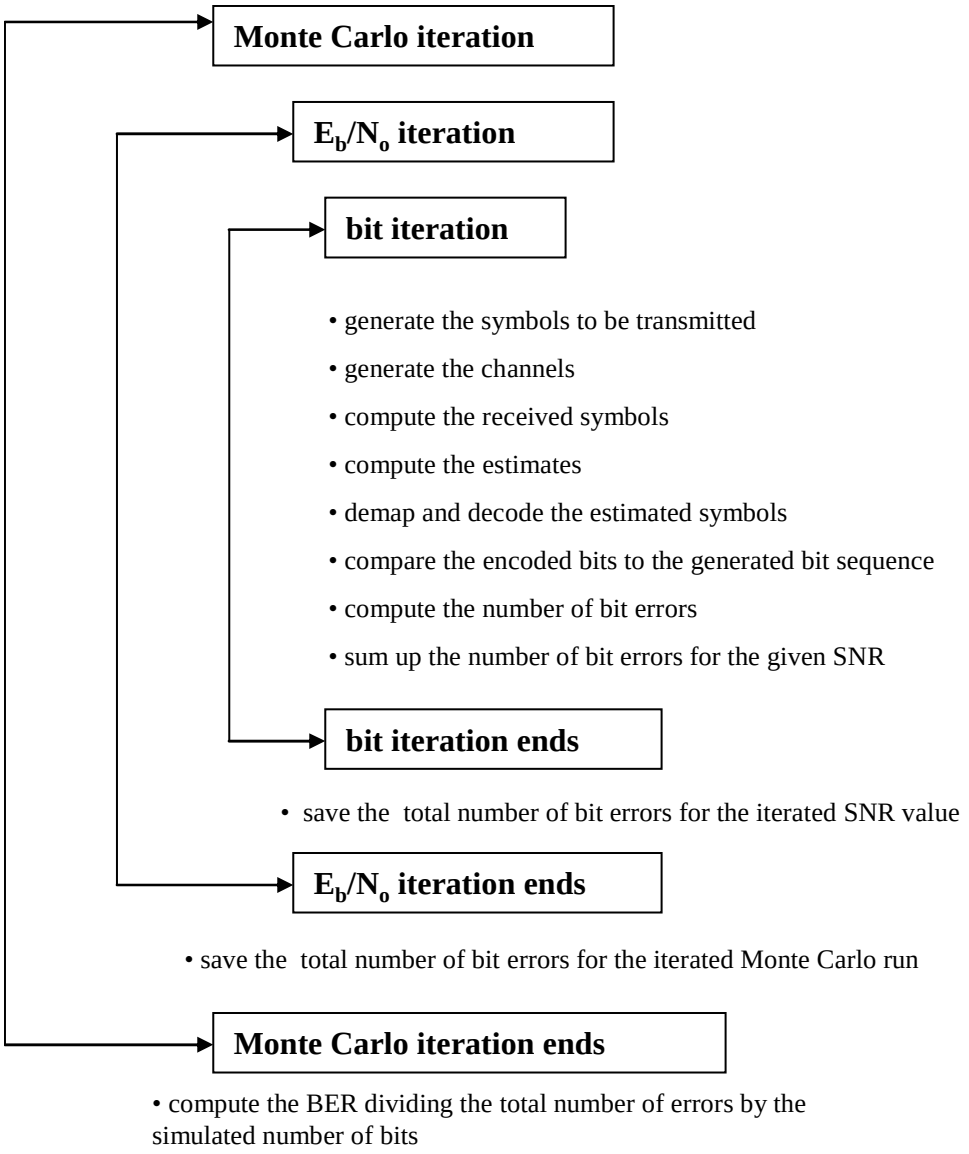

Figure 29. A Conceptual Diagram of the Iterations for the Outer Functions

C. EXPLANATIONS OF THE SUB-FUNCTIONS

While generating the outer codes, both Matlab's built-in and user constructed functions were used. Here, we explain the important functions used in the code.

randint.m is the Matlab's built-in function generating random bits "0" or "1" with equal probability.

convenc.m is the Matlab's built-in function which convolutionally encodes the randomly generated bits. The configuration of the convolutional encoder can be changed in the channel encoder section.

bin_2_mary.m converts the convolutionaly-encoded bits to *m*-ary symbols. The resulting sequence of this function is a vector with decimal numbers representing the symbols in the given constellation.

dmodce.m is the Matlab's built-in function which makes the *m*-ary mapping operation. Decimal numbers, representing the symbols in the constellation, are turned into complex numbers.

ifft_802_16.m takes a 192-symbol block sequence and creates an OFDM symbol. The function, organizes the information symbols as specified in the IEEE 802.16a standard (see Figure 15 and Table 6). Prior to the IFFT operation, the guard and pilot subcarriers are set to zero. After the IFFT operation, the function copies the desired CP length elements and adds them to the beginning of the output of the IFFT block. The CP length can be controlled by the variable 'Tg_rate' which is the optional guard ratio T_g / T_b . The guard ratio can be chosen as $1/4, 1/8, 1/16$ or $1/32$. The resulting CP length will be proportional to the FFT size 256. The output of the function is the baseband representation of an IEEE 802.16a OFDM symbol.

SUI_model.m generates a 3×1 complex vector including three-tap values of a SUI channel. All six SUI channel parameters are saved in this function. The function generates the channel tap values using the desired SUI index (1 to 6) and the directivity of the antenna (omni or 30° directional antenna).

SUI_model_resample.m holds the delay spread values for all six SUI channels. The function takes a 3 tap SUI channel and samples it with the desired sampling frequency.

create_mimo_channel.m generates the channels for a 2×2 system. The function calls *SUI_model.m* four times and generates the uncorrelated four paths of the 2×2 MIMO channel matrix. Next, the correlated channel is computed using the fading com-

ponents of the four SUI channels and the desired correlation coefficients (ρ_t and ρ_r). The complete correlated MIMO channel is computed with adding the fading component to the fixed component. The diagram shown in Figure 9 gives the steps taken in the function. Lastly, the function *SUI_model_resample.m* is called to sample the four MIMO paths with the desired sampling frequency.

create_miso_channel.m generates the channels for a 2×1 system. The steps taken in generating the correlated MISO channel are similar to those for the function *create_mimo_channel.m*.

create_simo_channel.m generates the channels for a 1×2 system. The steps taken in generating the correlated SIMO channel are similar to those for the function *create_mimo_channel.m*.

add_noise.m generates a sequence of complex random numbers chosen from a normal distribution with zero mean and desired noise variance. The dimension of the generated sequence is the same as the sequence that noise will be added.

fft_802_16.m takes the received OFDM symbol, removes the CP, takes the FFT and organize the information carriers. The output is a sequence with dimensions 1×192.

freq_res_info_carriers.m computes the frequency response of the corresponding 192 information subcarriers. The information subcarrier allocation is identical to the functions *ifft_802_16.m* and *fft_802_16.m*

non_causal_filter.m is used in decoding equations when a non-causal filter operation is needed.

ddemodce.m is the Matlab's built-in function which makes the *m*-ary demapping operation. The function takes the computed estimated complex sequences and demaps them to decimal numbers, representing the symbols in the constellation.

mary_2_bin.m converts the decimal number to bits by using the desired constellation size.

Vitdec.m is the Matlab's built-in function which makes the Viterbi decoding algorithm. In the simulation, the function is configured for hard decision decoding.

LIST OF REFERENCES

1. S. Mudulodu and A. Paulraj, "A Transmit Diversity Scheme for Frequency Selective Fading Channels," *Proceedings of the IEEE Global Telecommunications Conference, 2000,* Vol. 2, pp. 1089-1093, November 27, 2000.

2. A. Paulraj, R. Nabar and D. Gore, *Introduction to Space-Time Wireless Communications,* Cambridge University Press, Cambridge, United Kingdom, 2003.

3. G. Stuber, J. R. Barry, S. W McLaughlin, Y. LI, M. A. Ingram and T. S. Pratt, "Broadband MIMO-OFDM Wireless Communication," *Proceedings of IEEE,* Vol. 92. No.2, pp. 271-293, February 2004.

4. S. M. Alamouti, "A Simple Transmit Diversity Technique for Wireless Communications," *IEEE Journal on Select Areas in Communications,* Vol. 16, No. 8, pp. 1451-1458, October 1998.

5. J. G. Proakis, *Digital Communications,* pp. 822-823, McGraw Hill, New York, 2001.

6. H. Bolcskei and A. J. Paulraj "Space-Frequency Coded Broadband OFDM systems," *Proceedings of the IEEE Wireless Communications and Networking Conference,* Vol. 1, pp. 1-6, September 2000.

7. K. F. Lee and D.B. Williams, "A Space-Frequency Transmitter Diversity Technique for OFDM Systems," *Proceedings of the IEEE Global Telecommunications Conference, 2000,* Vol. 3, pp. 1473-1477, November 27, 2000.

8. E. Lindskog and A. Paulraj, "A Transmit Diversity Scheme for Channels with Intersymbol Interference," *Proceedings of IEEE International Conference on Communications, 2000,* Vol. 1, pp. 307-311, June 18, 2000.

9. K. Mehrotra and I.V. McLoughlin, "Time Reversal Space-Time Block Coding with Channel Estimation Errors," *Proceedings of the Fourth Pacific Rim Joint Conference on Information, Communications and Signal Processing,* Vol. 1**,** pp. 617-620, December 15, 2003.

10. Institute of Electrical and Electronics Engineers, 802.16a, Air Interface for Fixed Broadband Wireless Access Systems—Amendment 2: Medium Access Control Modifications and Additional Physical Layer Specifications for 2–11 GHz, 1 April 2003, http://ieeexplore.ieee.org, last accessed 17 November 2004.

11. V. Erceg, K.V.S Hari and M. S. Smith, "Channel Models for Fixed Wireless Applications," IEEE 802.16 Broadband Wireless Access Working Group Report - 03/01, June 2003, http://ieee802.org/16, last accessed 17 November 2004.

12. Z. Liu, Y. Xin and G. B. Giannakis, "Space-Time-Frequency Coded OFDM Over Frequency-Selective Fading Channels," *IEEE Trans. on Signal Proc.,* Vol. 50, No. 10, pp. 2465-2476, October 2002.

13. H. R. Anderson, *Fixed Broadband Wireless System Design*, p. 92, Wiley, West Sussex, England, 2003.

14. Y. Wang, "Analysis of Spatial Fading Correlation for different Antenna Array," *Proceedings of the IEEE Wireless Communications and Networking Conference, 2004*, Vol. 2, pp. 700-704, March 21, 2004.

15. T. S. Rappaport, *Digital Communications*, pp. 205-209, Prentice-Hall, Upper Saddle River, New Jersey, 2002.

16. H. Bolcskei, G. Gesbert, and A. J. Paulraj "On the Capacity of OFDM-based Spatial Multiplexing Systems," *IEEE Transactions on Communications,* Vol. 50, No. 2, pp. 225-234, February 2004.

17. A.Y. Erdogan, *Analysis of the Effects of Phase Noise and Frequency Offset in Orthogonal Frequency Division Multiplexing (OFDM) Systems*, Master's thesis, Naval Postgraduate School, Monterey, California, March 2004.

18. S. B. Wicker, *Error Control Systems for Digital Communication and Storage*, pp. 290-303, Prentice-Hall, Upper Saddle River, New Jersey, 1995.

19. J. Wang, M. K. Simon, M. P. Fitz and K. Yao "On the Performance of Space-Time Codes over Spatially Correlated Rayleigh Fading Channels," *IEEE Transactions on Communications,* Vol. 52, No. 6, pp. 877-881, June 2004.

20. J. Tsai, R. M. Buehrer and B. D. Woerner "Spatial Fading Correlation Function of Circular Antenna Arrays With Laplacian Energy Distribution," *IEEE Communication Letters,* Vol. 6, No. 5, pp. 178-180, May 2002.

21. M. Chiani, M. Z. Win and A. Zanella "On the Capacity of Spatially Correlated MIMO Rayleigh-Fading Channels," *IEEE Transactions on Information Theory,* Vol. 49, No. 10, pp. 2363-2370, October 2003.

22. D. Gu and C. Leung "Performance Analysis of a Transmit Diversity Scheme in Spatially Correlated Fading with Imperfect Channel Estimation," *Proceedings of the IEEE Pacific Rim Conference on Communications, Computers and Signal Processing,* Vol. 1, pp. 111-114, August 2003.

23. V. Tarokh, H. Jafarkhani and A. R. Calderbank “Space-Time Block Coding for Wireless Communication: Performance Results,” *IEEE Journal on Select Areas in Communications*, Vol. 17, No. 3, pp. 451-460, March 1999.

24. V. Tarokh, H. Jafarkhani and A. R. Calderbank “Space-Time Block Codes from Orthogonal Designs,” *IEEE Transactions on Information Theory*, Vol. 45, No. 5, pp. 1456-1467, July 1999.

THIS PAGE INTENTIONALLY LEFT BLANK

INITIAL DISTRIBUTION LIST

1. Defense Technical Information Center
   Ft. Belvoir, Virginia

2. Dudley Knox Library
   Naval Postgraduate School
   Monterey, California

3. Chairman, Code EC
   Department of Electrical and Computer Engineering
   Naval Postgraduate School
   Monterey, California

4. Professor Murali Tummala, Code EC/Tu
   Department of Electrical and Computer Engineering
   Naval Postgraduate School
   Monterey, California

5. Professor Roberto Cristi, Code EC/Cx
   Department of Electrical and Computer Engineering
   Naval Postgraduate School
   Monterey, California

6. Halil Derya Saglam
   Koru Mah. 499.Sok. No=I/2, Birlikkent Sitesi
   Cayyolu, Ankara, TURKEY